ChemBioEng Reviews

Overview of the Mechanism of Degradation of Pharmaceuticals by Persulfate/Peroxysulfate Catalysts

Excel O. Anjorin[1,2,3], **Moses O. Alfred**[2,3],*, **Babajide Sotunde**[2,3], **Esther A. Nnamani**[2,3], **Ajibola A. Bayode**[3], **Emmanuel I. Unuabonah**[2,3], **Brigitte Helmreich**[4], **Martins O. Omorogie**[2,3,4],*

Abstract

The leaching of pharmaceutical ingredients into water bodies poses an escalating threat, demanding urgent remediation strategies. Among several techniques advanced for their remediation, advanced oxidation methods utilizing persulfate (PS) and peroxymonosulfate (PMS) stand out as promising avenues for pharmaceutical degradation in wastewater. This article consolidates the research on photocatalytic degradation of pharmaceutical contaminants, focusing on PMS-based photoactive composites, and elucidates their efficacy in removing active pharmaceutical ingredients from water. Moreover, it delineates alternative techniques for activating PS and PMS, providing a holistic understanding of the field's advancements. By outlining research limitations and knowledge gaps, this review underscores the imperative for further investigation and innovation in pharmaceutical wastewater treatment.

Keywords: Peroxymonosulfate, Persulfate, Pharmaceuticals, Photocatalysis, Water

Received: December 01, 2023; *revised:* May 06, 2024; *accepted:* July 11, 2024

DOI: 10.1002/cben.202300079

1 Introduction

Pharmaceuticals have been significantly deployed to treat a plethora of sicknesses over the decades and are still presently used. However, their use has plagued our environment, particularly water bodies, with seemingly toxic residues, which has aroused the curiosity of many scientists to investigate how detrimental these toxic residues are, as well as develop remediation strategies for water bodies contaminated by animals [1]. Investigations conducted over the years have identified some pharmaceuticals that pose much harm to the environment. These pharmaceuticals include drugs used for the treatment of epilepsy, lowering blood lipids, depression, hormones, allergies, pains, bacterial infection, and high blood pressure [2].

These pharmaceuticals have been identified in wastewater effluents from households, manufacturing hubs, animal rehabilitation centers, drug-producing companies, and health centers [3, 4]. These effluents potentially leach into soils and, consequently, ground and surface water [5], and thus pose the risk of diseases to man and other living organisms in the environment [6]. Various studies have revealed that the treatment of pharmaceutical pollutants in water bodies may require different protocols due to variations in the physical and chemical properties of active pharmaceutical ingredients (APIs), sewage composition, and configuration of wastewater treatment plants (WWT). Some APIs are not easily degraded in nature and exhibit a "pseudo-persistence" nature that renders conventional biological and chemical treatment methods inefficient [7, 8]. Some of these pseudo-persistence APIs include antibiotics and

---

[1] Excel O. Anjorin
Department of Integrated Science Education, Federal College of Education (Technical) Akoka, P. O. Box 269, Yaba, Lagos 100001, Nigeria.

[2] Excel O. Anjorin, Dr. Moses O. Alfred (alfredm@run.edu.ng), Babajide Sotunde, Esther A. Nnamani, Prof. Emmanuel I. Unuabonah, Dr. Martins O. Omorogie
https://orcid.org/0000-0001-9697-2960 (omorogiem@run.edu.ng, mo.omorogie@tum.de)
Environmental Science and Technology Unit, African Centre of Excellence for Water and Environment Research (ACEWATER), Redeemer's University, PMB 230, Ede 232101, Nigeria.

[3] Excel O. Anjorin, Dr. Moses O. Alfred, Babajide Sotunde, Esther A. Nnamani, Dr. Ajibola A. Bayode, Prof. Emmanuel I. Unuabonah, Dr. Martins O. Omorogie
Department of Chemical Sciences, Redeemer's University, PMB 230, Ede 232101, Nigeria.

[4] Prof. Dr. Brigitte Helmreich
https://orcid.org/0000-0003-4224-3329, Dr. Martins O. Omorogie
Chair of Urban Water Systems Engineering, Technical University of Munich (TUM), Am Coulombwall 3, 85748 Garching, Germany.

Phase II metabolites of parent APIs, and their resistance to treatment increases in their concentrations in WWT [9].

This, thus, necessitates the search for advanced technologies for the effective removal of pharmaceuticals in wastewaters [10]. Biological and physical treatment methods like adsorption, ultrafiltration, and coagulation have been employed in previous years to remove organic pollutants from water. However, with less significant success and much cost implications. Advanced oxidation processes (AOPs) have been found to be more environmentally friendly in the removal of all kinds of contaminants. In addition, they are more efficient and less expensive as a treatment method. The deployment of advanced oxidation processes is characterized by the release of hydroxyl, sulfate, and superoxide radicals that help to mineralize or lower the concentration of contaminants [11]. Additionally, the use of AOPs is characterized by the ease of implementation, high efficiency, and environmental adaptability and capability of oxidizing a broad spectrum of contaminants. They have been broadly used to remove refractory pollutants [11]. However, they are limited by the need for an operational acidic condition and the unpredictability of hydrogen peroxide (H_2O_2) [12].

Most researchers perceive the sulfate radical-AOPs (SR-AOPs) to be a favorable AOP for water and wastewater treatment [13]. According to many studies, SRs can be produced by activating peroxymonosulfate (PMS) or peroxysulfate through suitable heating, ultraviolet (UV) radiation, or transition metal activation [14–16]. In comparison to hydroxyl-based AOPs, SR-AOPs have elevated reduction-oxidation (REDOX) potential, require more moderate reaction pH conditions (2.0–8.0), an extended half-life (30–40 s), and an increased oxidation capacity in both carbonate buffer solutions and phosphate buffer solutions [17–19]. Several reviews exist on SR-AOPs. For instance, Honarmandrad et al. [19] discussed the details of the mechanism of SR-AOPs and applications for antibiotics degradation, and another review explains the role of $^1O_2$ in SR-AOPs to help with its reasonable utilization [20] and several others. However, to the best of our knowledge, there is a dearth of information on the selective interaction of SR on target pharmaceutical compounds. Meanwhile, this information is essential to the understanding and prediction of the degradation mechanism and no information on their mineralization potential. Therefore, this study intends to review previous investigations carried out on the use of persulfate (PS)- and peroxysulfate-based photoactive composites for the degradation of pharmaceuticals in water, particularly from the perspective of the mineralization mechanism. This is important because the ultimate desire of a degradation process is to optimize the conversion of the contaminants to their mineral components to facilitate the reduction of their environmental toxicity. Furthermore, understanding the mineralization mechanism would help researchers design the process to be more sustainable in terms of time and cost.

2 Advanced Oxidation Processes Based on SRs

Advanced oxidation processes based on SR provides a viable alternative, especially for applications in the degradation of pharmaceuticals in water [21–26]. Some of the advantages of the SR-based advance oxidation process are highlighted as follow:

1. The oxidation of $SO_4^{-\bullet}$ (2.5–3.1 V) is higher than $^{\bullet}OH$.
2. SR reacts more selectively and efficiently via electron transfer with organic compounds that contain unsaturated bonds or aromatic π electrons. By contrast, $^{\bullet}OH$ is a non-selective radical and may also react with the diverse background constituted by hydrogen abstraction or electrophilic addition [26, 27].
3. SR reacts efficiently with organic compounds over a wide pH range of 2.0–8.0, reaching a higher standard oxidation potential than hydroxyl radical (HR) at neutral pH [25].
4. The half-life of SR is supposed to be 30–40 μs, which enables the radical to have more stable mass transfer and better contact with target compounds than HRs, whose half-life is 20 ns [24, 26].

However, on its own, this process is not economically viable for full-scale real-life application, and it is majorly activated with the use of UV radiation. However, these challenges can be mitigated when activation is achieved through the combination of heterogeneous photocatalysis.

Hydrogen peroxide eclipsed PS as a strong oxidizing agent for advanced oxidation processes. For several years, advanced oxidation processes were described as a process that produces HRs. Notable processes associated with AOPs include Fenton and Fenton-related processes and the use of light (i.e., photolysis) and heterogeneous catalysis as a means of remediation for polluted sites and wastewater treatment. In addition, the use of ozone (O_3) in combination with H_2O_2 (i.e., ozonation) and oxidation using permanganate were included in this description [28]. In the same vein, in situ chemical oxidation processes for the treatment of polluted subsurface sites were, at first, also included in this description. However, the detection of $S_2O_8^{2-}$ (i.e., PS ion) and the understanding of its significance as a strong starting material or initiator for the generation of sulfate ion radical for use in advanced oxidation process was eclipsed by H_2O_2 and the affiliated HR. Before the earliest claim of the making of persulfuric acid was put forward by Berthelot in 1878 [29], hydrogen peroxide had been recognized as a strong oxidizing agent for many years. There was severe contention about the oxidizing ability of persulfuric acid, owing mainly to the fact that many scientists then believed that the demonstrated oxidizing characteristics of this compound could be traced to H_2O_2. Nevertheless, the exhaustive research carried out by Marshall [29] was able to establish the novel compound discovered to be persulfuric acid and the salt associated with the compound as PS (which was a sulfur oxyanion containing additional oxygen than the typical sulfate).

3 PS- and Peroxysulfate-Based Photocatalysts

While conventional AOPs are situated on HR oxidation of organics, recently, SR advanced oxidation processes have become keenly considered by researchers as a novel substitute to conventional advanced oxidation processes. Following the first publication in this area of study by Anipsitakis and

Dionysiou [30], a revived interest by scientists in this area of research has brought about a lot of publications highlighting the use of different $SO_4^{\bullet-}$ generating methods and its efficiency as treatment in the degradation of a plethora of organic contaminants. Some unique benefits of SR advanced oxidation processes give validation to their application. First, $SO_4^{\bullet-}$ has the potential to efficiently oxidize a broad spectrum of organics due to its REDOX potential, which falls within the range of 2.5 and 3.1 V. Second, $SO_4^{\bullet-}$ reactivity is not dependent on pH, compared to the effectiveness of the elimination of organics by $^{\bullet}$OH, which reduces with an increase in pH (e.g., Fenton reaction works best at a pH value of 3.0). $SO_4^{\bullet-}$ tends to be considerably more reactive at neutral pH than $^{\bullet}$OH [30].

This particular advantage of $SO_4^{\bullet-}$ oxidation processes is most important when dealing with increased flow rates or highly buffered wastewater because the need for extra chemicals to adjust the pH of the wastewater is circumvented. The possibility of $SO_4^{\bullet-}$ reacting with organic contaminants is higher than $^{\bullet}$OH due to its increased lifetime in aqua solution and its rapid reaction rates [31]. Based on research on various contaminants, researchers have established in different published works that degradation effected using $SO_4^{\bullet-}$ shows better rate of mineralization, compared to $^{\bullet}$OH [32–35]. Another reason adduced for this superior ability in the mineralization of contaminants is the self-scavenging effect, which has little significance for SRs, thereby, allowing for the creation of greater radical concentrations in water. This, thereby, enhances the kinetics of the reaction of highly loaded wastewater. In addition, $SO_4^{-\bullet}$ has a superior selectivity in comparison to $^{\bullet}$OH [33, 36]. This characteristic makes it possible to use $SO_4^{-\bullet}$ to attack particular functional groups that have been identified to be the cause of contaminants' molecular ecotoxicity. The precursors usually used for generating $SO_4^{-\bullet}$ are PMS and PS. The SR is generated by activating these precursors [37].

3.1 PS and PMS

PS occurs in the form of a salt (i.e., $Na_2S_2O_8$ or $K_2S_2O_8$), while PMS only occurs stable as a triple salt (i.e., $2KHSO_5$, $KHSO_4$, K_2SO_4). PMS is produced commercially and can be purchased using the names Oxone and Caroat. Different activation methods have been put forward for the activation of PMS and peroxysulfate. It includes the addition of a transition metal catalyst [38], the use of elevated temperature (i.e., thermal elevation) [39], and the use of UV light or ultrasound [40]. Despite the achievement of encouraging outcomes in the area of SR-AOPs, the number of papers that addresses SR-AOPs is lesser than that for conventional advanced oxidation processes. There is still a need for comprehensive research on SR-AOPs to completely comprehend the process involved in its mechanism for degradation. The components of the wastewater, the activation procedure utilized, and the process conditions determine to a large extent the kind of dominant radicals (i.e., $SO_4^{\bullet-}$ or $^{\bullet}$OH) that will be generated. It has a great impact on the mechanism of degradation occurring. Despite the performance of quenching studies in some initial investigations, the reaction between various classes of organics and radicals is still sketchy. Ammonium PS, a frequently utilized PS, is particularly effective in hair bleaching products as it assists in the breakdown of natural hair pigments, enabling desirable lightening or color removal outcomes [41]. PSs serve as widely employed initiators for polymerizing different monomers, including acrylates and vinyl monomers. PSs decompose when exposed to a reducing agent or heat, leading to the formation of radicals that initiate the polymerization process. The application of PSs as initiators for polymerization is highly prevalent in manufacturing polymers, coatings, adhesives, and composites.

Although it has been demonstrated that particular functional groups that cause molecular environmental toxicity of contaminants are targeted by SRs, there is still a need to look into the extent of hazard associated with the by-products generated from SR advanced oxidation processes in comparison with conventional advanced oxidation processes for various categories of specific contaminants. Most of the data presently available regarding SR-AOPs are mostly generated from experiments carried out in the laboratory. The effect of this technology when used in a continuous mode has not been really investigated. Because SR-AOPs use precursor chemicals that contain sulfur, the hydrosphere could be impacted by the leftover sulfates that may linger after treatment.

Also, the strength or durability of SR-AOPs in removing contaminants in actual wastewater with variation in time and composition has not been achieved. Presently, the most effective medium of activation to produce $SO_4^{-\bullet}$ uses hazardous metals like Co, and this will result in the need for an extensive and expensive expulsion of these metal ions from wastewater after applying SR-AOPs technology. Hence, they cannot be used as homogeneous catalysts. The ability to use these metals as heterogeneous catalysts in immobilized form is still unclear due to a lack of adequate research on their characteristics (i.e., regarding how stable they are, their tendency to impact color or befoul, and their leaching tendency). In addition, improvement in immobilized catalysts is one other important aspect to be considered. There is still the need to explain in detail the systems that make it possible for the combined effects that are seen when merging SR-AOPs with conventional AOPs. In this regard, the type of radicals used will play a significant role.

3.1.1 Chemistry of PS-Based Oxidation

PS-based advanced oxidation processes differ from conventional advanced oxidation processes in their chemistry [42] and operation mechanism. In relation with other conventional advanced oxidation processes that utilize $^{\bullet}$OH as the main oxidant, PS-based advanced oxidation processes possess benefits that include the production of $SO_4^{-\bullet}$, which has an elevated REDOX potential of 2.5–3.1 V_{NHE} in comparison with 1.9–2.7 V_{NHE} for $^{\bullet}$OH [43]; an extended half-life between 30 and 40 µs in comparison with 20 ns for $^{\bullet}$OH, and therefore can spread out farther to interact with contaminants for degradation [44]; generation of $SO_4^{-\bullet}$ that can interact effectively with organic compounds with less reliance on the conditions of operation [19]; and they are easily obtained and cheap to convey and store [45, 46].

Table 1. Comparison of physical—chemical properties, reactivities, and main oxidants for peroxymonosulfate (PMS) and PS [51].

	PMS	PS
Standard reduction potential [E°]	1.82 V_{NHE}	2.08 V_{NHE}
Peroxide bond dissociation energy	377 kJ mol^{-1}	92 kJ mol^{-1}
Molar absorption coefficient at 248 nm	19.1 $M^{-1}.cm^{-1}$	27.5 $M^{-1}.cm^{-1}$
Acid dissociation constant [pKa]	9.30	−3.50
Reactivity toward nucleophiles	Effective oxygen atom transfer reactions to nucleophiles, such as X^- and HCO_3^- (leading to secondary oxidant formation)	Negligible (stable at excess background anions)
Reactivity toward radicals	pH-dependent $pH < pKa_2 = 9.30$ (HSO_5^-) $k(SO_4^{-\bullet}) < 10^5\ M^{-1}.s^{-1}$ $k(^\bullet OH) = 1.70 \times 10^7\ M^{-1}.s^{-1}$ $pH > pKa_2 = 9.30$ (SO_5^{2-}) $k(SO_4^{-\bullet}) < 10^5\ M^{-1}.s^{-1}$ $k(^\bullet OH) = 2.10 \times 10^9\ M^{-1}.s^{-1}$	$k(SO_4^{-\bullet}) = 1.20 \times 10^6\ M^{-1}.s^{-1}$ $k(^\bullet OH) < 10^6\ M^{-1}.s^{-1}$
Main oxidant during activation by base and quinones	O_2 resulting from accelerated self-decay of PMS	$SO_4^{-\bullet}$ resulting from PS reduction
Preferred activation method	Electron-transfer-based activation (e.g., catalysis with transition)	Energy-transfer-based activation (e.g., thermolysis, photolysis)

NHE, Normal hydrogen electrode.

Due to these benefits, PS-based advanced oxidation processes have generated great interest among scientists for their use in the remediation of pollutants in the environment. There has been a corresponding increase in the number of scientific papers published on PS-based AOPs. PS, which includes PMS and peroxydisulfate, can be activated into $SO_4^{-\bullet}$ through different channels, which include the use of light, also referred to as photolysis, the use of heat, also referred to as thermolysis, the use of sound, also referred to as sonolysis, through heterogeneous catalysis (using transition metals like Co, Fe, Mn-based oxides, titanium dioxide, and other catalysts), and through homogeneous catalysis [45, 47, 48]. However, due to the high energy needed, it is practically impossible to use thermal activation or ultrasound activation in massive wastewater treatment. However, photolysis or activation using photons is considered a mild and economical means of applying light as the energy source for environmental remediation [49]. Solar radiation (i.e., energy from the sun) at 1366 W m^{-2}, comprises 3 % UV light, 44 % visible light, and 53 % infrared. It has excellent benefits, compared to other energy sources because it is unpaid for; does not impact pollution (i.e., clean); and not just easily replenished but limitless [50].

The chemistry of PS is described by its oxidizing ability with a REDOX potential second only to ozone (i.e., O_3) for frequently used oxidizing agents in advanced oxidation processes. However, the oxidative reactions of PS are usually sluggish when no catalyst is used and at room temperature. The activation of PS to generate the highly oxidizing SR (i.e., $SO_4^{-\bullet}$) involves the homolytic breaking (i.e., cleavage) of the O—O bond. The energy needed for the breaking of the O—O bond can be obtained from thermolysis (i.e., from heat), photolysis (i.e., from UV radiation), radiolysis (i.e., from ionizing radiation), or through catalysis (i.e., from chemical electron transfer) [52] (Tab. 1).

3.2 Activation of PS and PMS

The use of thermal energy, UV radiation, alkaline treatment, and metal ion reactions are the major routes for activating PS and PMS. There exists a significant difference between $SO_4^{-\bullet}$ generated through the various methods of activation of PS and PMS, concerning their general working structure (i.e., mechanisms), channels of operation (i.e., pathways), and REDOX potential. Therefore, summarizing the effectiveness of various methods of PS and PMS activation is vital to itemizing the crucial goals of producing SR. Tab. 2 summarizes the mechanism, strength, and setbacks of some of these activation methods.

3.2.1 Physical Activation Approaches

Thermal Activation

Despite its high energy demand, thermal activation has been identified as one of the most efficient conventional methods for activating PS and PMS to produce SR ions [53]. The research work carried out by Ji et al. [54] found that PS could not be activated at room temperature for the efficient degradation of tetracycline (TTC). On the other hand, with an increase in the temperature to 70 °C within 30 min of reaction set to operate within an acidic condition, a total degradation of TTC is observed. It clearly shows that increased temperature contributes significantly to the generation of $SO_4^{-\bullet}$. A corresponding outcome was also obtained by [53], in which it was observed that an increment in the temperature from 20 to 75 °C resulted in marked improvement in the decomposition of PS, $SO_4^{-\bullet}$ production, and concomitant growth in acidic by-product generated. The thermal activation of PS and PMS in degradation processes offers several advantages. It has been shown to be effective in the rapid degradation and

Table 2. Summary of the different activation methods.

Activation method	Mechanism	Advantage	Setback
Thermal	Raising the temperature facilitates the activation of PS and PMS, leading to the generation of sulfate radical (SR) ions	Enhances the oxidation efficiency of organic contaminants at elevated temperatures. Promotes the generation of highly oxidative species that can react with a variety of organic pollutants. It can be used in a variety of environment. It is easily combined with other techniques	High energy demand
Alkali	Alkali activation involves the addition of NaOH or KOH to raise the pH level, leading to the hydrolysis of PS molecules and the formation of superoxide radicals	Increases electron transfer efficiency	The use of alkali for activation may involve the generation of by-products and the need for careful pH control to ensure efficient activation. It cannot be combined easily with other activation techniques
UV	UV irradiation activates oxidants like PMS, leading to the production of SRs for the degradation of pollutants	Efficient in activating PMS for pollutant degradation, especially in the UV wavelength range. Provides sufficient energy for the scission of the peroxo bond in PMS structure, leading to the generation of SRs	It requires energy, which brings additional cost to the process. UV could interact with the contaminants to generate more toxic by-products
Ultrasound	Ultrasonication generates free radicals ($SO_4^{\bullet-}$ and $HO^{\bullet}$) by increasing the number of active cavitation bubbles and facilitating the fast activation of PMS	Considerable efficiency in activating PMS for pollutant degradation. Increases the number of active cavitation bubbles, leading to fast activation of PMS and generation of SRs	Difficulty with reactor scale-up poses a great challenge to its real-life application. In addition, the reactor setup and operation cost make the process uneconomical, compared to other activation types. Produces a greater amount of hydrogen radicals than SRs, which can affect the overall efficiency of the process
Catalytic	Heterogeneous catalysts play a crucial role in activating PMS by providing a surface for the reaction, leading to the generation of SRs for pollutant degradation. This involves the transfer of conduction electrons from the photocatalysts to PMS, leading to the generation of SRs for pollutant degradation	Offers a unique approach to activating PMS through electron transfer processes. Heterogeneous catalysts provide a surface for the reaction to occur, enhancing the activation of PMS and the generation of SRs for pollutant degradation. The process offers a catalytic approach to activating PMS, potentially improving the efficiency of the process compared to non-catalytic methods	The catalyst's efficiency can be decreased by interfering with different agents, such as contaminants and inorganic compounds, in the reaction medium

mineralization of organic pollutants, such as azo dyes, humic acid (HA), salicylic acid, and caffeine [55]. The synergistic effect of thermal and alkali activation has been found to enhance the degradation of contaminants in coal chemistry industry wastewater [56]. Furthermore, the development of novel photothermal methods for PS activation, such as the use of solar photothermal and near-infrared light-to-heat conversion, has been shown to significantly improve the degradation of micropollutants in water purification processes [57]. These studies collectively demonstrate the potential of thermal activation in PS and PMS degradation processes.

Activation Method

The increased energy of UV radiation has established it as a widely acknowledged and effective means of activating PS and PMS. PS and PMS activation using UV light is fundamentally based on the breaking of the O─O bond. As shown in Eq. (1), two $SO_4^{-\bullet}$ radicals are produced after activation of PS, while $SO_4^{-\bullet}$ and $^{\bullet}OH$ are produced by PMS activation. This is due mainly to the asymmetric structure. Under UV activation, there is a possibility for the conversion of a fraction of the produced $SO_4^{-\bullet}$ into $^{\bullet}OH$ resembling the process observed during heat activation (Eq. 3), which is pH-dependent.

$$S_2O_8^{2-} + hv \rightarrow 2SO_4^{\bullet-} \quad (1)$$

$$HSO_5^{-} + hv \rightarrow SO_4^{\bullet-} + {}^{\bullet}OH \quad (2)$$

$$SO_4^{\bullet} + H_2O \rightarrow SO_4^{2-} + {}^{\bullet}OH + H^{+} \quad (3)$$

Based on the research conducted by [58], it was observed that $SO_4^{-\bullet}$ acted as the main radical when the pH was less than

7.0, but once the pH increased to 9.3, it would undergo conversion to OH^- as indicated in the study by [59]. In recent research, UV/PS utilization has been reported for the degradation of challenging organic compounds. Extensive investigations have demonstrated that UV/PS exhibits a higher capacity for the oxidation of organic pollutants than UV/PMS. This disparity in oxidizing potential is attributed to the elevated quantum yield observed in UV/PS as described by [60]. The use of UV light to activate PS and PMS is hindered by its limited presence in solar light, constituting only a small fraction of approximately 3–5 %. To overcome the constraints, recent studies have explored the utilization of visible and solar light for photoactivation, in addition to UV radiation [61, 62].

Ultrasound Activation

Two primary mechanisms that underlie the activation of PS/PMS by ultrasound involve the presence of cavitation bubbles as follow; (a) the formation of SR by the homolysis of the O—O bond under high temperatures (approximately 5000 K) and pressures, resembling the energy-induced mechanisms observed in heat and UV activation, and (b) through the influence of cavitation bubbles, water molecules undergo decomposition, forming HR and hydrogen radicals (Eq. 4) [46, 63], and the generation of HR and hydrogen radicals via the decomposition of water molecules under the action of cavitation bubbles (Eq. 4). According to an investigation by Wang and Wang [46], ultrasonic activation produced a greater amount of HR than SR, particularly in the case of PS. The recombination rate of HRs is impeded at high temperatures due to the low dissociation energy of the O—O bond in H_2O_2 as noted by Von Sonntag [64]. Consequently, under ultrasonic conditions, the concentration of HRs can attain the millimolar level.

$$H_2O \rightarrow {}^{\bullet}OH + {}^{\bullet}H \tag{4}$$

Numerous studies have shown that ultrasound activation of PS effectively generating SR at room temperature, but its efficiency decreases at higher temperatures, particularly at 65 °C [28, 65]. Like heating activation, ultrasound activation of PS also suffers from high cost and massive energy consumption. In addition, to achieve ultrasound activation of PS, alkaline conditions ($pH > 10.0$) are required, which generate a large amount of $SO_4^{\bullet-}$, superoxide (O^{2-}), and OH^- through Eqs. (5)–(7) [65].

$$S_2O_8^{2-} + 2H_2O \overset{OH^-}{\rightarrow} HO_2^- + 2SO_4^{2-} + 3H^+ \tag{5}$$

$$S_2O_8^{2-} + 2HO_2^- \rightarrow SO_4^{\bullet-} + SO_4^{2-} + 2H^+ + 2O_2^{-\bullet} \tag{6}$$

$$SO_4^{\bullet-} + OH^- \rightarrow SO_4^{2-} + OH^{\bullet} \tag{7}$$

3.2.2 Chemical Activation Approaches

Activation of PS/PMS Using Alkali

PS/PMS can be activated using alkaline solution. Alkali activation of PS/PMS is a prevalent in situ technique that involves the addition of NaOH or KOH to raise the pH level (usually above pH 11.0) [45, 63]. In the activation process, the hydrolysis of a PS molecule leads to the formation of $H_2O_2^-$ (i.e., H_2O_2 anion) and consequently to superoxide radicals (O_2^-) as shown in Eqs. (8) and (9) [45, 46, 63].

$$S_2O_8^{2-} + 2H_2O \rightarrow HO_2^- + 2SO_4^{2-} + 3H^+ \tag{8}$$

$$S_2O_8^{2-} + HO_2^- \rightarrow SO_4^{\bullet-} + SO_4^{2-} + H^+ + O_2^{-\bullet} \tag{9}$$

In addition, as illustrated in Eq. (10), under alkaline conditions, $SO_4^{\bullet-}$ can be transformed into ${}^{\bullet}OH$ [46].

$$SO_4^{\bullet-} + OH^- \rightarrow SO_4^{2-} + OH^{\bullet} \tag{10}$$

The use of alkali to activate PMS follows a pathway that is completely different. According to [66], singlet oxygen and superoxide anion radicals are the main reactive oxygen species (ROS) in the alkali/PMS system, and ${}^{\bullet}OH$ may be produced through the hydrolysis of HSO_5^- as illustrated in Eqs. (11)–(15).

$$HSO_5^- \rightarrow SO_5^{2-} + H^+ \tag{11}$$

$$HSO_5^- + H_2O \rightarrow HSO_4^- + H_2O_2 \tag{12}$$

$$SO_5^{2-} + H_2O \rightarrow SO_4^{2-} + H_2O_2 \tag{13}$$

$$H_2O_2 \rightarrow HO_2^- + H^+ \tag{14}$$

$$H_2O_2 \rightarrow 2OH^{\bullet} \tag{15}$$

According to Qi et al. [66], the HR mentioned earlier reacts with excess H_2O_2 to form superoxide anion radicals (Eqs. 16 and 17), which are then transformed into singlet oxygen and hydroxide ions as shown in Eq. (18). The superoxide anion radical can also produce H_2O_2 and singlet oxygen (Eq. 19), and singlet oxygen can be generated through self-disintegration as illustrated in Eq. (20) [46]. The HR and superoxide anion radical would then be converted to singlet oxygen and hydroxide ions (Eq. 18). In contrast, the superoxide anion radical can also generate H_2O_2 and singlet oxygen (Eq. 19) [66]. In addition, singlet oxygen can be generated via self-decomposition (Eq. 20) [46].

$$H_2O_2 + {}^{\bullet}OH + H^+ = 2OH^{\bullet} + H_2O \tag{16}$$

$$HO\,_2^{-\bullet} \rightarrow H^+ + O_2^{-\bullet} \tag{17}$$

$${}^{\bullet}OH + O_2^{-\bullet} \rightarrow O_2 + OH^- \tag{18}$$

$$2H^+ + 2O_2^{-\bullet} \rightarrow O_2 + H_2O_2 \tag{19}$$

$$HSO_5^- + SO_5^{2-} \rightarrow HSO_4^- + SO_4^{-\bullet} + O_2 \tag{20}$$

Alkali-activated PS/PMS is less efficient and has a longer degradation time than heating, UV, and metal activations as reported by Xia et al. [42] and Devi et al. [67]. Furthermore, Zhao et al. [68] demonstrated that activating PS by alkali method showed a lower degree of effectiveness for degrading polycyclic aromatic hydrocarbons.

Activation of PS Using Direct UV Radiation

The degradation of contaminants using a direct reaction between PS or PMS with pollutants is, to some extent, sluggish and most times, undesirable [45]. Due to the elevated energy of UV light, elaborate investigations have found that irradiation using UV can effectively activate PS and PMS [69, 70]. PS and PMS can be activated by making use of UV irradiation with wavelength ranging from 200 to 400 nm because UV radiation within this wavelength region is considered friendly to the ecosystem and economical. Activation of PS using UV irradiation can, therefore, lead to the production of SR, which is used to remove contaminants with a corresponding increased proportion of efficiency devoid of concomitant discharge of metallic catalyst.

Dye Sensitization Activation of PS

The visible portion of sunlight has been reported to be approximately 44 %, with its wavelength ranging from 400 to 800 nm, while the UV amount of the sun is said to be 3 %. Due to the higher percentage of the visible light spectrum of sunlight and to effectively utilize sunlight, a significant amount of interest has been raised to see the possibility of developing PS-based AOPs that can be activated by the visible spectrum of sunlight [50]. However, due to the inadequacy of the photon energy contained in visible light, compared to UV light, it cannot be used to directly activate PS and PMS.

It is, however, worthy of note that visible light can be used in the excitation of a few distinct photosensitive organic dyes, which can then be used for the activation of peroxydisulfate and PMS to produce $SO_4^{-\bullet}$ and $^\bullet OH$. The comprehensive mechanism of activation is as follows: Electrons contained in the dye molecules are excited from the highest occupied molecular orbital (HOMO) to the lowest unoccupied molecular orbital (LUMO) by radiation from visible light. PS then receives the excited electrons to produce active $SO_4^{-\bullet}$ and $^\bullet OH$. Therefore, the dye molecules take on a dual role of acting as the photosensitizer and the substrate to be removed or reduced. In addition, the dye that was excited by the photons from visible light can equally abstract electrons by oxidizing contaminants and resulting in the dye molecules' decolorization.

Activation of PS Using Dye Sensitization-Mediated Homogeneous Catalysis

Transition metal ions (e.g., Fe^{2+}, Co^{2+}, Cu^{2+}, Mn^{2+}, Ce^{3+}, Ru^{3+}, etc.) can be used to activate PS and PMS. This activation is carried out via a one-electron transfer method [71–73]. An increase in the oxidation rate of pollutants is enabled during homogeneous catalytic activation of PS due to the observed inconsequential mass transfer limitation between phases [44]. However, disadvantages noticeable in typical Fenton reaction (e.g., low long-term performance due to reduced performance of the previously oxidized metal) can also be observed when activation of PS by homogeneous transition metal ion is carried out in the absence of light [44]. The rate-inhibiting step usually reduces the oxidized metal ion back to the active species.

The low rate constant affects the catalytic activity, as the reduction of oxidized metal ion to the active species serves as the rate-determining step [74]. A critical challenge in PS-based processes involving homogeneous catalytic activation is the need to speed up the REDOX cycling of the metal ion activator. To overcome this limitation, dye sensitization has been utilized to facilitate the REDOX cycling of the metal ion activator in homogeneous PS activation systems. In the context of dye sensitization-assisted homogeneous catalytic activation, the interaction between transition metal ions and photosensitive dye molecules (D) leads to the formation of complexes that contain metals as depicted in Eq. (21). In the presence of visible light, the photosensitive dye molecules absorb photons and convert them into electrons, which are then transferred from the dye molecules to the transition metal catalyst. This electron transfer event facilitates the regeneration of the catalyst ($M^{(n+1)+} \rightarrow M^{n+}$) and leads to the formation of oxidized dye (D^{*+}) as indicated in Eq. (22). Upon regeneration, the active species activate PS or PMS, leading to the generation of $SO_4^{-\bullet}$ and $OH^\bullet$ radicals (Eqs. 23–25).

Furthermore, the photo-excited dye is capable of oxidizing pollutants through electron abstraction, causing the dye to lose its color. The activation of PS or PMS was successfully achieved using a dye-assisted Co^{2+} process as demonstrated in the research conducted by Chen et al. [72]. The transfer of electrons from photo-excited Acid Orange 7 (AO7) molecules to oxidized Co^{3+} (Eqs. 21 and 22) facilitates the regeneration of Co^{2+} for catalytic pollutant removal. Sensitized dye accelerates catalyst regeneration, leading to enhanced activation of PS or PMS, decreased catalyst usage, reduced metal precipitation, and minimized sludge formation.

$$M^{(n+1)+} + \mathrm{Dye} \rightarrow M^{(n+1)+} - D \tag{21}$$

$$M^{(n+1)+} - D + hv \rightarrow M^{n+} + D^{*+} \tag{22}$$

$$M^{n+} + S_2O_8{}^{2-} M^{(n+1)+} \rightarrow SO_4{}^{\bullet-} + SO_4{}^{2-} \tag{23}$$

$$M^{n+} + HSO_5{}^{-} \rightarrow M^{(n+1)+} + SO_4{}^{\bullet-} + OH^{-} \tag{24}$$

$$M^{n+} + HSO_5{}^{-} \rightarrow M^{(n+1)+} + SO_4{}^{2-} + {}^\bullet OH \tag{25}$$

$$SO_4{}^{-\bullet} \text{ or } {}^\bullet OH + \mathrm{Pollutants} \rightarrow \mathrm{Products} \tag{26}$$

The efficacy of light-assisted homogeneous catalytic PS-based advanced oxidation processes (AOPs) for contaminant degradation is accompanied by a range of limitations that curtail their wide-ranging application. These limitations include the potential for the precipitation of metallic sludge ions, which demands the collection, treatment, and disposal of the sludge, thereby raising the operating costs [19], and the addition of metal salts can lead to the presence of anions, such as SO_4^{2-} and Cl^-, which may hinder the activation of PS due to their radical quenching effects [75, 76].

Activation of PS Using Dye Sensitization-Aided Heterogeneous Catalysis

The development of heterogeneous systems has offered a solution to the limitations of homogeneous activation when activating PS. Through heterogeneous PS activation, the production of iron sludge can be minimized, and the detrimental effects of salts can be avoided [77]. The activation of PS through heterogeneous catalysis occurs through two major reaction pathways that include the interaction between PS and surface metal species, and the leaching of metal ions from the heterogeneous catalysts, facilitating the homogeneous activation of PS [13, 78].

Despite the presence of homogeneous PS activation in heterogeneous processes, its heterogeneous activation pathway is of paramount significance. A decline in catalytic activity can be observed in metal oxide catalysts during heterogeneous catalytic activation of PS due to the inadequate restoration of oxidized metal to its reduced state [79]. Dye sensitization is integrated into the heterogeneous catalytic activation of PS to enhance the reformation of active metal species. Similar to homogeneous systems, heterogeneous catalytic activation also follows a comparable mechanism. As highlighted by Eqs. (23) and (24) from the study conducted by Gao et al. [80], these equations illustrate how the electron transfer from photo-excited sensitizers can expedite the catalytic cycle of $\equiv M^{(n+1)+}$ to $\equiv Mn^{+}$ (with M denoting the metal element) in a transition metal oxide catalyst, thereby facilitating the heterogeneous activation of PS.

Ligand-to-Metal Charge Transfer (LMCT) Activation of PS

In the context of PS and PMS activation, an alternative approach to photosensitization known as LMCT exists; this operates independently of dye sensitization. In contrast to dye sensitization, LMCT ligands cannot directly absorb visible light. Instead, these ligands are absorbed onto a catalyst's surface, creating photosensitive charge transfer (CT) complexes that include a metal component. By harnessing light, the photosensitive complexes enable the transfer of charges from the adsorbed ligands' HOMO to the catalyst, a phenomenon referred to as the LMCT process [41, 81, 82]. The application of LMCT has extended to both homogeneous and heterogeneous activation of PS and PMS, offering promising prospects in both systems.

Homogeneous Activation of PS through LMCT

There is widespread documentation of scientific investigations showing that the use of homogeneous catalytic activation via transfer of charge from ligand to metal in the presence of UV [83] or radiation from the sun [84] can considerably improve the elimination and the mineralization of different organic contaminants. As mentioned earlier, the swift oxidation of the active metal ion species serves as the rate-determining step in the homogeneous catalysis process for PS activation. The rapid conversion of $M^{(n+1)+}$ back to M^{n+} is accountable for the significant enhancement in catalytic performance observed in LMCT-aided homogeneous catalytic activation.

This conversion process gives rise to $SO_4^{-\bullet}$ and $^{\bullet}OH$ radicals through the LMCT pathway. Using iron-based catalysts for instance, iron III (Fe^{3+}) and iron II (Fe^{2+}) can bind to the ligands to produce light-sensitive metal-containing complex. The LMCT sensitizers do not possess light-absorbing properties, but the metal-containing CT complexes they generate can capture light. The absorption of light and the subsequent conversion of photons into excited electrons by these complexes results in the regeneration of Fe^{2+} from Fe^{3+} (Eq. 27) [85]. Activation of PS or PMS by the photogenerated ferrous ion in the presence of light produces ($SO_4^{-\bullet}$) and ($^{\bullet}OH$) radicals, which act in concert to degrade organic contaminants.

$$Fe^{3+} - L + hv \rightarrow Fe^{2+} + L^{*} \tag{27}$$

PS Activation through Heterogeneous LMCT

The use of LMCT has expanded to include the heterogeneous activation of PS and PMS. Certain ligands exhibit the capacity to establish surface CT complexes with semiconductors such as TiO_2. Under normal circumstances, due to its significant band gap, TiO_2 requires UV light for activation. Nevertheless, Zhang et al. [82] proposed that LMCT-mediated photocatalysis can activate PMS by TiO_2 under visible light. The surface CT complex, in the presence of visible light, serves as a mediator for the transfer of electrons from the adsorbate's HOMO to the semiconductor's conduction band (CB). This mechanism triggers the catalytic activation of PS or PMS and subsequently produces SRs [81].

Activation of PS Via Photocatalysis

PS and PMS can be activated through photocatalysis to facilitate the oxidation of contaminants as stated by Wang et al. [43]. Photoactivated electrons and holes produced by the photocatalyst initiate the activation of photocatalysis. The photocatalyst directly transfers electrons with the photosensitizer or activates indirect electron transfer as part of the reaction mechanism.

4 Parameters Affecting PS- and PMS-Based Photocatalysis

There are various factors affecting PS- and PMS-based photocatalysis. They include photocatalyst dosage, PS dosage, initial contaminants concentration, co-existing inorganic and organic matter, and solution pH.

4.1 Photocatalyst Dosage

The role of photocatalyst dosage in the degradation of organic pollutants during PS and peroxysulfate photocatalysis can be comprehended by studying the PS-assisted TiO_2-based photocatalysis [86]. Increasing the catalyst dose yielded a favorable result [87–91]. In their research on the degradation of ibuprofen (IBP) using the TiO_2/UV/PS system, Hu et al. found that varying the TiO_2 dose (10 to 40 mg L^{-1}) led to a linear relationship between the pseudo-first-order rate and TiO_2 dosage. This phenomenon is attributed to the concurrent elevation in the quantity of electron-hole (e^-/h^+) pairs and ROS such as $SO_4^{-\bullet}$ and $^{\bullet}OH$, which correspondingly escalate with the increase in TiO_2 dosage. The removal efficiency of Bisphenol A (BPA) in the D35-TiO_2/g-C_3N_4/Vis/PS system was found to exhibit a significant increase when the catalyst dose was elevated from 0.2 to 1.0 g L^{-1} [92].

Adding a higher catalyst dosage can contribute to the presence of more reactive sites and the induction of photo-generated electrons to activate PS, facilitating the generation of a large quantity of ROS for the degradation of BPA. However, the growth trend of BPA degradation efficiency diminishes when the catalyst dosage is increased from 1.0 to 1.5 g L^{-1} due to the limited quantity of PS. Initially, there was an improvement in the removal efficiency of pollutants as the catalyst dosage increased, but later on, a decrease was observed [66, 93–95].

Possible explanations for the decreased efficiency at excessive catalyst dosing include the overcrowding of catalyst particles can lead to increased light reflection and scattering, reducing the effective surface area available for catalytic reactions [96, 97], and too large a quantity of catalyst dosage can promote the gathering and self-association of catalyst particles, thereby diminishing the number of available reactive sites [94, 95, 97, 98]. Thus, the elevation of catalyst dosage often improves the degradation efficiency of pollutants in PS-assisted photocatalysis. Nonetheless, it is essential to judiciously assess the catalyst dosage to achieve a suitable trade-off between efficiency and cost.

4.2 PS Dosage

The degradation efficiency of organic contaminants is influenced by the dosage of PS, just like the effect of catalyst dosage. Utilizing the TiO_2/light/PS system as an example, it is evident that the photo-induced electrons can be efficiently captured by PS, leading to the formation of $SO_4^{-\bullet}$, which serve as the primary ROS responsible for the degradation of organic pollutants. The relationship between PS dosage and process efficiency can be explained by considering two scenarios. First, a rise in the degradation efficiency of organic contaminants, but as the PS dose increased, there was a subsequent decline [88, 94–96, 98, 99].

By increasing the dosage of PS in the TiO_2/light/PS system, additional $SO_4^{-\bullet}$ radicals are formed, contributing to the accelerated oxidative degradation of organic contaminants. However, when introducing excessive amounts of PS, it leads to the in situ generation of $SO_4^{-\bullet}$ radicals, which can be captured by PS molecules as shown in Eqs. (28) and (29). Consequently, this leads to a decrease in the efficiency of decontamination. Also, an incremental improvement in the degradation efficiency of pollutants was observed as the PS dosage increased [90, 91, 100–102]. The removal efficiency did not exhibit a noticeable increase when the PS dose was high, likely because of the limited dosage of the catalyst [89–91].

$$SO_4^{\bullet -} + S_2O_8^{2-} \rightarrow S_2O_8^{\bullet -} + SO_4^{2-} \quad (28)$$

$$SO_4^{\bullet -} + HSO_5^{-} \rightarrow SO_5^{\bullet -} + SO_4^{2-} + H^{+} \quad (29)$$

Table 3. Influence of solution pH on different organic pollutants degradation in TiO_2/light/persulfate (PS) system [19].

Model pollutants	PS	pH range	Optimal pH	Ref.
Safranin O	PS	1.0, 3.0, 6.2, 9.0, 11.0, 13.0	13.0	[91]
Tetrabromobisphenol A	PS	9.0, 10.0, 11.0, 12.0	12.0	[96]
Sulfaclozine	PS	7.0, 11.0	11.0	[100]
Ibuprofen (IBP)	PS	3.0, 5.0, 6.0, 8.0, 10.0	6.0	[88]
Aniline	PS	4.0, 7.0, 10.0,	4.0	[99]
Imazalil	PS	3.0, 6.5, 10.0	3.0	[87]
Perfluorooctanoic acid	PMS	3.0, 5.0, 7.0, 9.0	3.0	[107]
BPA	PMS	3.0, 3.98, 5.0, 7.0, 9.0, 11.0	3.0	[105]

4.3 Initial Pollutant Concentration

When maintaining a steady light intensity, catalyst dosage, and PS dose in PS-assisted TiO_2-based photocatalysis, the production of ROS, particularly $SO_4^{-\bullet}$ and $^{\bullet}OH$, at the catalyst's surface can be presumed to remain unchanged. Hence, when the initial concentration of pollutants is elevated, the consumption of ROS will also increase, ultimately resulting in a reduced degradation efficiency [87, 90, 95, 98, 101–105]. Additionally, the presence of pollutants like 2,4-dichlorophenoxyacetic acid and acetaminophen at high concentrations on the catalyst surface can hinder the passage of light, thereby diminishing the interaction between light and catalyst, which in turn reduces the generation of ROS [97, 104].

As a result, it is imperative to consider the pollutant concentration adequately when considering the feasibility of using PS/PMS-assisted photocatalysts for wastewater treatment.

4.4 The pH of the Solution

In $SO_4^{-\bullet}$-based oxidation systems, the pH of the solution plays a vital role in eliminating of organic pollutants, mainly due to its impact on the catalyst's surface charge, PS decomposition, ROS formation, and the existing molecular state of organic pollutants [19, 44]. The relationship between solution pH and the degradation of diverse organic pollutants using pure TiO_2 as the photocatalyst and PS as the oxidant is outlined in Tabs. 2 and 3.

Specific pollutant's most effective degradation efficiency is determined by whether the pH is acidic or alkaline. It is worth noting that the pH at the point of zero charge (pHpzc) for TiO_2 is approximately 6.3. Thus, the surface of TiO_2 carries a negative charge when the solution pH exceeds 6.3, but it undergoes a shift to a positive charge when the solution pH is approximately 6.3. Tab. 2 reveals that during the degradation of IBP, the strength of the electrostatic interaction between TiO_2 and $S_2O_8^{2-}$ was higher at pH 3.0 than at pH 6.0. Surprisingly, despite the stronger interaction, the rate of IBP degradation was lower at pH 3.0 than at pH 6.0.

This disparity can be attributed to the fact that IBP remained unchanged at pH 3.0, resulting in the absence of an electrostatic interaction between TiO_2 and IBP. At pH 8.0 and pH 10.0, a decrease in the degradation rate was observed because of the repulsion between negatively charged TiO_2 and IBP, as well as PS. According to the findings of [32, 106], the interplay between $SO_4^{-\bullet}$ and $^{\bullet}OH$ radicals were as follows: $SO_4^{-\bullet}$ was the primary radical at $pH < 7.0$, both $SO_4^{-\bullet}$ and $^{\bullet}OH$ coexisted at $pH = 9.0$, and $^{\bullet}OH$ became the primary radical at $pH > 9.0$. At pH 4.0, TiO_2 and aniline exhibited an electrostatic repulsion, whereas at pH 10.0, an electrostatic attraction was observed. Interestingly, the degradation efficiency of aniline was higher at pH 4.0 than at pH 10.0. This discrepancy can be attributed to the predominant influence of $SO_4^{-\bullet}$, which played a more crucial role in aniline degradation at pH 4.0, compared to the $^{\bullet}OH$ [99].

The reactivity of the $^{\bullet}OH$ with perfluorooctanoic acid is relatively low, resulting in a better degradation efficiency of perfluorooctanoic acid at pH 3.0 than at pH 9.0 [107]. The optimal elimination effectiveness of sulfaclozine was achieved at pH 11.0, mainly because the $^{\bullet}OH$ radical emerged as the primary ROS responsible for the degradation of sulfaclozine [100]. The degradation of tetrabromobisphenol in an alkaline aqueous solution [96] reveals an escalating degradation efficiency as the pH was increased from 9.0 to 12.0. At elevated pH levels, a swift equilibrium between $^{\bullet}OH$ and its conjugate base $O^{-\bullet}$ could be achieved (Eq. 30). Consequently, both the $^{\bullet}OH$ and $O^{-\bullet}$ radicals are engaged in the degradation of tetrabromobisphenol.

$$^{\bullet}OH + OH- \leftrightarrow O^{-\bullet} + H_2O \qquad (30)$$

4.5 Coexistence of Inorganic and Organic Substances

In natural water bodies and practical wastewater, the coexistence of organic substances such as HA and effluent organic matter, as well as diverse inorganic ions including Cl^-, HCO_3^-, CO_3^{2-}, NO_3^-, SO_4^{2-}, and $H_2PO_4^-$, can disrupt the $SO_4^{\bullet-}$ radical-induced reactions, resulting in an unpredictable outcome for the removal of target pollutants from water [19, 108, 109]. A comprehensive study on the effect of these natural components on pollutant degradation in PS/peroxysulfate-assisted photocatalysis can facilitate the real-world application of this technology in the treatment of polluted water. Inorganic anions such as Cl^-, HCO_3^-, CO_3^{2-}, NO_3^-, and $H_2PO_4^-$ can be captured by $SO_4^{\bullet-}$ and $^{\bullet}OH$ radicals, characterized by their high REDOX potentials, leading to the formation of less reactive daughter radicals [19, 44, 110]. Introducing inorganic anions typically has an adverse effect on the removal efficiency of organic pollutants in PS-assisted photocatalysis, resulting in reduced effectiveness in water treatment [88, 89, 97, 102, 105].

However, it is important to acknowledge that certain inorganic anions positively impact the efficiency of the process. For example, in the degradation of BPA using the TiO_2/Vis/PMS system, the presence of Cl^- ions can increase the removal efficiency of BPA by facilitating the production of active chlorine species ($Cl^{\bullet}$, $Cl_2^{-\bullet}$, and $ClOH^{-\bullet}$) through reactions with $SO_4^{-\bullet}/^{\bullet}OH$, thereby promoting the degradation of BPA [105]. In the TiO_2/UV/PS system, Bekkouche et al. [91] found that the inclusion of NO_3^- can improve the degradation rate of Safranin O. This enhancement is linked to the production of various free radicals ($NO_3^{\bullet}$, $NO_2^{\bullet}$, and $^{\bullet}OH$) in the presence of NO_3^- ions (Eqs. 31–33).

Additionally, it was observed that a higher initial concentration of anions results in a weakened inhibitory effect on the degradation efficiency. In the TiO_2/UV/PS system, the degree of inhibition in the degradation of IBP was observed to diminish when the Cl^- concentration was raised from 1 to 3 mM. This decrease in inhibition is due to the interaction between Cl^- ions and h^+ on the valence band (VB) of TiO_2. Consequently, the higher Cl^- concentration enables a greater number of electron (e^-) particles from the CB of TiO_2 to be involved in PS activation [88].

$$NO_3^- + h\nu \rightarrow \left[NO_3^-\right]^* \qquad (31)$$

$$\left[NO_3^-\right]^* \rightarrow NO_2^{\bullet} + O^{\bullet-} \qquad (32)$$

$$O^{\bullet-} + H_2O \rightarrow {}^{\bullet}OH + OH^- \qquad (33)$$

HA is a prominent type of natural organic matter (NOM) that is present in substantial amounts in natural water bodies and wastewater [86, 111]. Notably, HA can consume the $SO_4^{-\bullet}$ and $^{\bullet}OH$ radicals produced in AOPs [86]. Therefore, the presence of HA in AOPs tends to decrease the efficiency of target pollutant removal. Ding and Hu [88] conducted a study that revealed a substantial decrease in the degradation rate of IBP in a TiO_2/UV/PS system in the presence of HA.

Several reasons account for the decrease in the degradation rate of IBP in the presence of HA in the TiO_2/UV/PS system. First, HA functions as a UV light screen, causing a reduction of photons reaching the TiO_2 surface. Also, HA binds to the surface of TiO_2, thereby reducing the interaction between TiO_2 and PS. HA can capture the in situ generated $SO_4^{\bullet-}$ and $^{\bullet}OH$ radicals. Additionally, Bekkouche et al. [91] documented similar results on eradicating "Safranin O" in a TiO_2/UV/PS system. In contrast, a TiO_2/Vis/PMS system boosts the degradation efficiency of BPA by the presence of HA. This is attributed to the capacity of HA to be excited by visible light, resulting in the generation of e^- particles that transfer to the CB of TiO_2. These e^- particles participate in the reaction with PMS, producing extra $SO_4^{\bullet-}$ radicals, ultimately enhancing the degradation efficiency of BPA.

5 Application of PS- and PMS-Based Photocatalyst

5.1 Degradation of Pharmaceuticals in Water

The activation of PS and PMS for the degradation of pharmaceuticals in water has been explored through various methods [112] (Fig. 1). Jabbari et al. [113] demonstrated how PS can be applied to degrade diclofenac in water using the $O_3/UV/S_2O_8$ AOPs. The research findings showed how the integration of PS into UV/PS or ozone/PS systems enhances the treatment process

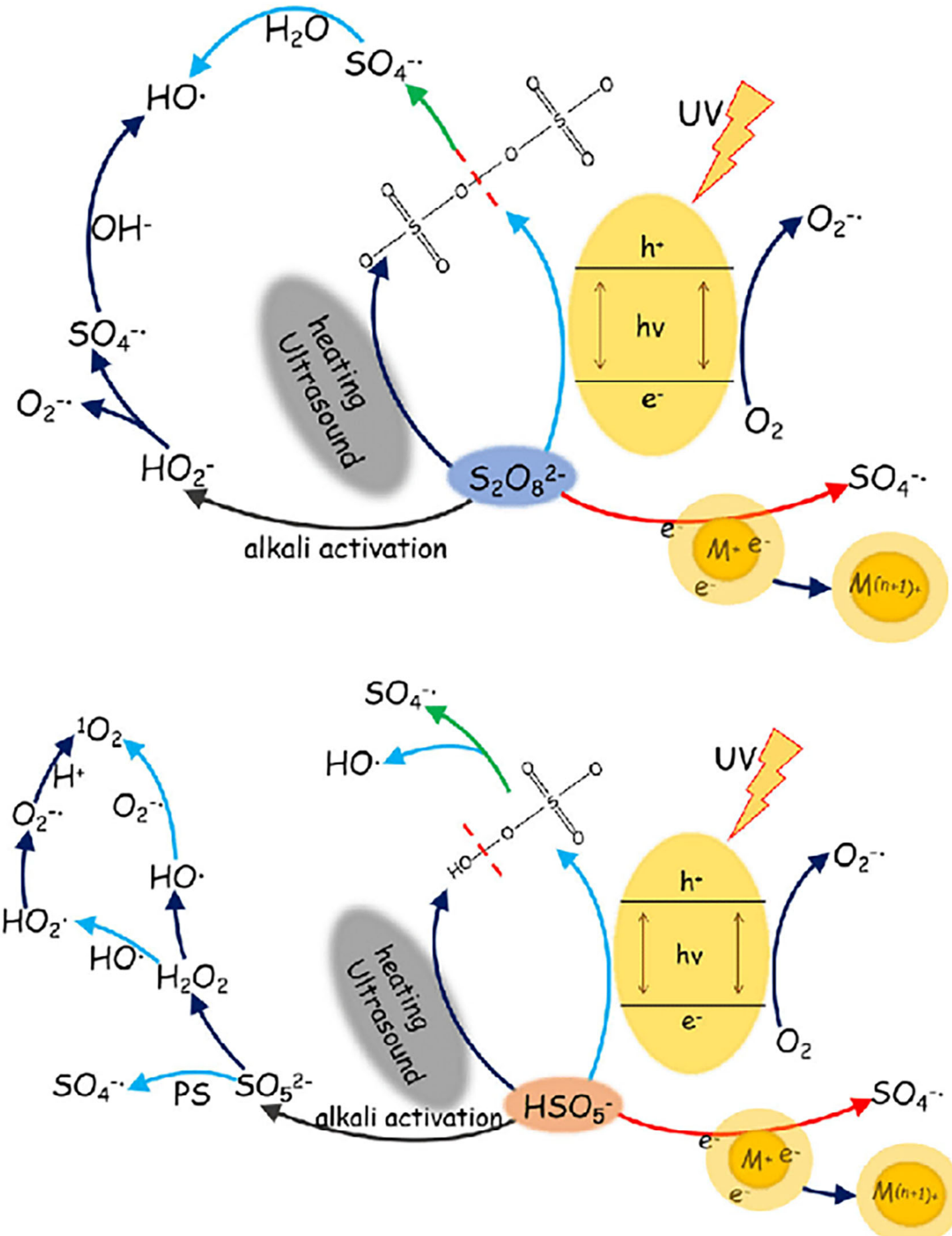

Figure 1. Generation of sulfate radical via PS/peroxymonosulfate activation under different reaction conditions [46].

by promoting the degradation and removal of pharmaceutical compounds in water. PS acts as an oxidizing agent, helping to break down the pharmaceutical compounds and facilitate their removal from the water. Fig. 2a,b shows a typical example of the stepwise mechanism for the degradation of diclofenac using PMS systems, and the mechanism of PS degradation of TTC, respectively.

Qin et al. [114] in their preliminary study on the integrated UV/ozone/PS process for efficient removal of atrazine (ATZ) (a chlorinated triazine systemic herbicide that is used to selectively control annual grasses and broadleaf weeds before they emerge) showed that the combination of UV, O_3, and PS demonstrated significant treatment efficacy, resulting in a notable increase in the rate of ATZ degradation. The k_{obs} value for

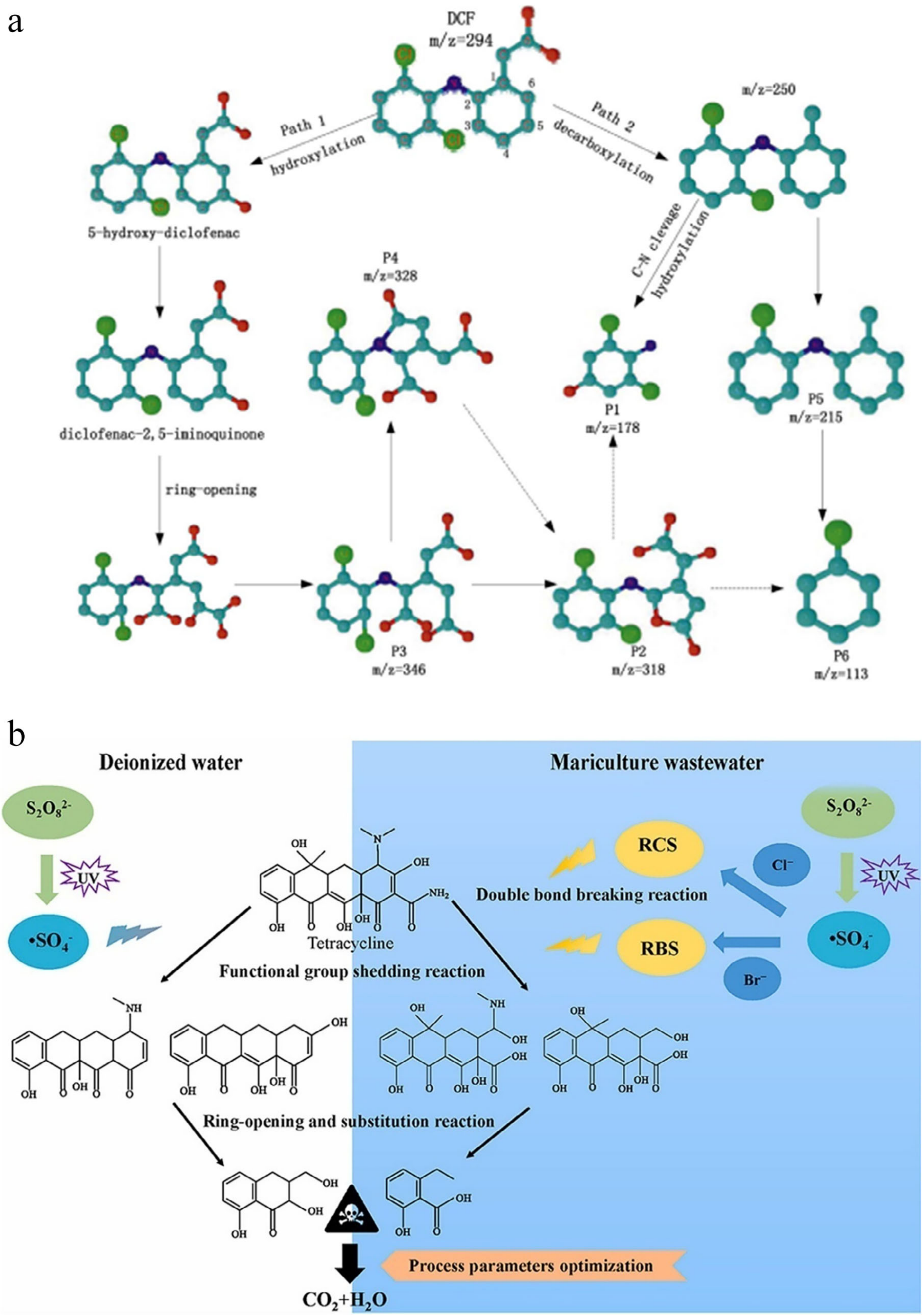

Figure 2. (a) UV-activated PS removal process for diclofenac [115]. (b) Mechanism of PS degradation of TTC [121].

ATZ degradation showed an 18.7-fold enhancement, compared to the O_3/PS treatment, a 3.3-fold enhancement, compared to the UV/O_3 treatment, and a 2.6-fold enhancement, compared to the UV/PS treatment. This integration of multiple treatment methods exhibited superior performance in degrading ATZ.

Yin et al. [115] applied the combination of CNTs and PS for the degradation of sulfamethoxazole. The presence of CNTs as activators promotes the generation of $SO_4^{-\bullet}$, which plays a crucial role in the degradation process. The research reveals that the degradation efficiency increases with higher CNT dosage and PS concentration. Additionally, the optimal pH range for efficient degradation was found to be slightly acidic. The findings contribute to the understanding of advanced oxidation processes for removing antibiotics from water systems and provide valuable insights for developing more efficient and sustainable water treatment methods.

Seidmohammadi et al. [116] explored the removal of metronidazole, a commonly used antibiotic, using ozone-activated PS in the presence of ultrasound. They found that the removal of metronidazole decreased by increasing the pH of the solution from 3.0 to 11.0. The removal rate of metronidazole depended on initial PS dosages and the highest removal rate was found in 500 mg L^{-1} (94.7 %), but in higher concentrations, the removal rate decreased. In the study by Wu et al. [117], the degradation of chloramphenicol in water was addressed through the combination of photocatalysis and PMS oxidation. A functional system was developed by combining strontium-doped lanthanum cobaltate with chlorine-doped carbon nitride, which was further coupled with PMS oxidation. The combined effect of PMS oxidation and photocatalysis was leveraged to great effect, as the composite material with an optimal 40 % strontium-doped lanthanum cobaltate loading achieved an impressive degradation rate of 95.6 % for chloramphenicol within 20-min duration.

5.2 Removal of Transformation Products

The study conducted by Gao et al. [118] appraised the use of PS as an effective method for targeting and removing transformation products from the degradation of sulfametazine in water. The research findings suggested that PS can effectively degrade transformation products, which are by-products that form during the breakdown of sulfamethazine in water. Applying PS can contribute to a more thorough removal of these compounds, ensuring a more comprehensive water treatment process.

5.3 Removal of BPA in Industrial Wastewater

The study conducted by Wang et al. [43] appraised the application of PS as a promising method for addressing the presence of BPA compounds in industrial wastewater, thereby aiding in environmental protection and sustainable practices. The research findings highlighted the potential of PS in treating industrial wastewater that contains BPA compounds. Using PS can mitigate the environmental impact of pharmaceutical manufacturing activities.

6 Mechanism of Degradation of Pharmaceuticals via PS/PMS AOPs

It is imperative to note that the specific mechanism and efficiency of PS activation for pharmaceutical degradation depend on factors such as the nature of the pharmaceutical compound, the choice of catalysts or activators, reaction conditions like pH, temperature, and the presence of other chemical constituents such as anions and scavengers in the system. Typically, the mechanism of the degradation of pharmaceuticals using SRs involves electron transfer, unlike HR, which requires hydrogen-atom abstraction reaction in tandem with electron transfer. The degradation and decomposition of organic pollutants by sulfate and HRs include different mechanisms (Tab. 4). It is noteworthy that $SO_4^{-\bullet}$ participates mainly in the outer space mechanism for electron transfer reaction [119, 120].

In a study conducted by Zhang et al., their finding showed that the main degradation pathway of TTC by UV/PS process was via functional group shedding and ring-opening reactions taking place sequentially by SR and HR. In the study, the degradation of TTC molecules in deionized water was divided into three paths (Fig. 3).

First, $SO_4^{-\bullet}$ selectively reacted with electron-rich groups (amide group, tertiary amine group, hydroxyl group, and double bond) and $OH^\bullet$ showed high activity for the olefin double bond. In the first pathway, the tertiary amine groups of TTC, then hydroxyl, methyl, and formamide were destroyed, and after the ring opening and substitution reactions, some intermediate products were produced. In the second pathway, the cyclo-addition of $OH^\bullet$ occurred through the loss of formamide, and methyl groups, followed by a series of ring opening and replacement reactions to produce other intermediate compounds. In the third pathway, the removal of carboxamide and the third amine group from TTC molecules and the production of intermediate products occurred. Finally, by using cyclo-addition of $OH^\bullet$ and demethylation reaction, the intermediate products were converted into small molecular products. Among the three degradation pathways, the electron-withdrawing groups, such as carbonyl and carboxyl, were not easily directly attacked. Still, they were continuously degraded by the gradual opening of the ring structure of TTC molecules [121].

Another study reported by Xiaoli et al. investigated the degradation of an antibiotic sulfadiazine (SD) by developing a novel ultrasound-enhanced heterogeneous (ultrasound/FeO/PS) system. First, the SR caused the oxidation of the amine group and produced nitro-SD derivatives, and by attacking the nitro-SD derivatives, the heterocyclic ring opens. In the second degradation path, SR caused direct oxidative cleavage of the S–N bond. The results of the ion chromatography tests revealed that formic acid, acetic acid, and some inorganic ions were the final products of SD decomposition [119]. Tab. 3 summarizes recent publications on the degradation mechanisms/pathways of selected pharmaceuticals in water.

PMS is applied in the aquaculture and fish farming to control the proliferation of bacterial, viral, and parasitic fish diseases. By effectively disinfecting water and equipment, PMS aids in maintaining a favorable and healthy environment for fish in aquaculture and fish farming operations [58]. The application

Table 4. Degradation pathways of selected pharmaceuticals in water.

Pharmaceuticals	Method of activation	Oxidizing agents	Degradation mechanism	Functional group attacked	Ref.
Carbamazepine	Gamma radiation/$S_2O_8^-$	SO_4^- SO_4^-, $OH^\bullet$	Electron transfer, hydroxylation of aromatic rings	Aromatic (benzene ring)	[145]
Diclofenac sodium	$Fe^{2+/}S_2O_8^-$, Fe^{2+}/H_2O_2 or Fe^{2+}/SO_4^-	SO_4^-, $OH^\bullet$	Hydroxylation, decarboxylation, dichlorination-cyclization, formylation, dehydrogenation, dechlorination-hydrogenation	Alkene, halocompounds, ketenimine, alkyne, carbon dioxide and alcohol	[146]
Tetracycline (TTC), oxytetracycline (OTC), and chlorotetracycline (CTC)	Thermo-activated $S_2O_8^-$ oxidation	SO_4^-, $OH^\bullet$	Demethylation, hydroxylation–oxidation and dehydration	Alkyl group, amide group, hydroxyl compound, and alkene group	[54]
Ciprofloxacin	Magnetic gamma $Fe_2O^{3-}MnO_2/S_2O_8^-$	SO_4^-, $OH^\bullet$	Hydroxyl group substitution	Hydroxyl group, amino group, piperazine ring opening, and formaldehyde compounds	[121]
IBP	$UV/S_2O_8^-$	SO_4^-, $OH^\bullet$	Decarboxylation and hydroxylation	IBP ring opening	[147]
Diclofenac	$UV/S_2O_8^-$	SO_4^-, $OH^\bullet$	Decarboxylation, dechlorination, and hydroxylation	Carboxyl group, chlorine atom and OH group	[147]
Naproxen	$UV/S_2O_8^-$	SO_4^-, OH^-	Decarboxylation and hydroxylation	Naphthalene ring opening, carboxyl and hydroxyl group	[147]
Lincomycin	Basolite F300 MOF/$S_2O_8^-$	SO_4^-, OH^-	Hydroxylation, soxidation, desulfurization, pyranose ring opening, and cleavage of the C—N bond		[148]

MOF, metal-organic framework; UV, ultraviolet radiation.

of PMS as an oxidizing agent in situ chemical oxidation technique enables the successful remediation of contaminated soils and groundwater, offering an effective solution. The powerful degradation abilities of PMS extend to a wide array of organic contaminants, including petroleum hydrocarbons, chlorinated solvents, and phenolic compounds [122]. The strong oxidizing capabilities of PSs make them popular in hair bleaching formulations.

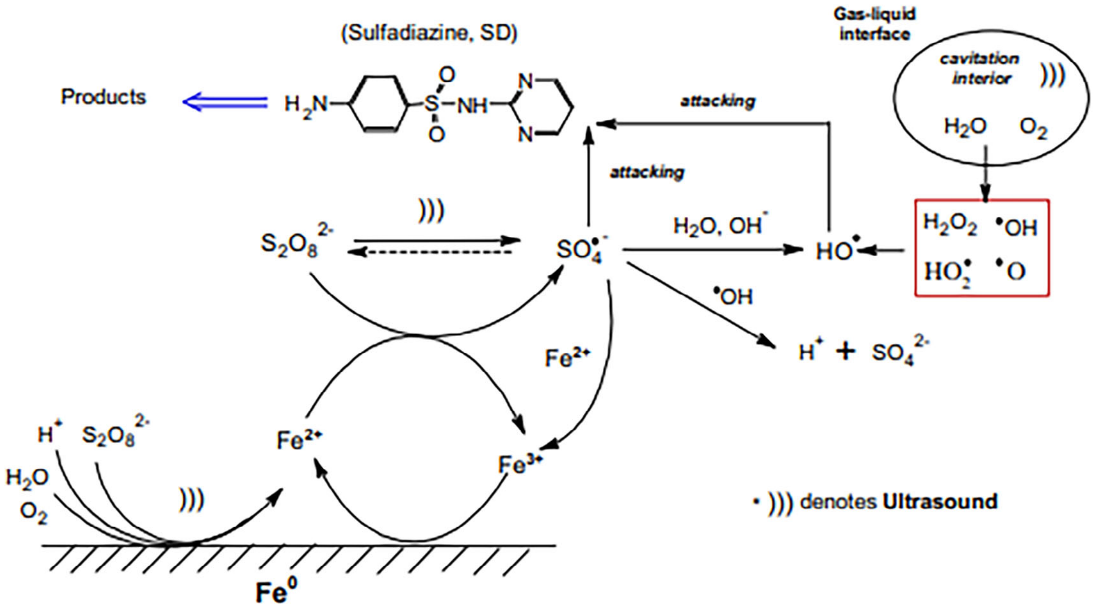

Figure 3. Ultrasound-enhanced heterogeneous (ultrasound/FeO/PS) system for removal of sulfadiazine (SD) [119].

7 Degradation versus Mineralization in PMS and PS AOPs

HRs and $SO_4^{\bullet-}$ stand as the principal oxidizing agents accountable for the enhanced efficacy of AOPs when juxtaposed with traditional treatment methodologies [123]. Consequently, AOPs are conventionally categorized into two classes: HR-AOPs and SR-AOPs, based on generating these superior oxidants. Compared to alternative AOPs, SR-AOPs exhibit many advantageous attributes, some of which have been documented in this review. SR-AOPs show notable selectivity, a high REDOX potential at near-neutral pH levels, readily available reactants like PS, and diminished reactant demand [124, 125]. These compelling attributes render SR-AOP an attractive choice for real-world applications. In addition, it is noteworthy that SR-AOPs exhibit comparatively restricted interference from NOM when contrasted with HR-AOP ($6.6 \pm 0.4 \times 10^3$ L.mg.C^{-1}.s $^{-1}$ for SR-AOPs, compared to HO$^\bullet$: $1.4 \pm 0.2 \times 10^4$ L.mg.C^{-1}.s $^{-1}$ for HR-AOP) [52].

Extensive research has underscored the remarkable advantages of employing PS and PMS oxidants for treating water containing high levels of NOM and various inorganic constituents. Notably, this approach reduces the formation of NOM-related by-products as compared to the use of H_2O_2 [34, 126]. In addition, as it relates to pollutant removal, investigations have consistently demonstrated that oxidation processes based on $SO_4^{\bullet-}$ exhibit superior or comparable performance when compared to $^\bullet$OH oxidation, particularly in terms of total organic carbon (TOC) removal and the enhancement of biodegradability [124, 127, 128]. Therefore, the primary limitations associated with HR-AOPs, such as susceptibility to matrix interference and the requirement for acidic pH conditions, can be substantially mitigated through the adoption of SR-AOPs while maintaining comparable activity levels [45].

In SR-AOPs, the principal radical species responsible for pollutant degradation is $SO_4^{\bullet-}$, although in certain instances, particularly during PMS activation, $^\bullet$OH also assumes a crucial role as contributors [129]. In contrast to HR-AOPs, SR-AOPs encompass a broader array of secondary oxidants, including $O_2^\bullet$, $^1O_2$, $^\bullet$OH, and $CO_3^{\bullet-}$ [45, 130]. The intricate interactions among various constituents within the water matrix, including NOM and inorganic anions, may result in either the scavenging of oxidants or the formation of secondary radicals, such as Cl$^\bullet$, Br$^\bullet$, and $CO_3^{\bullet-}$ [45]. These secondary radicals can also play a significant role in the degradation of pollutants.

Although, $SO_4^{-\bullet}$ and $^\bullet$OH share similar REDOX potentials, their chemical reactivity differs significantly. $SO_4^{\bullet-}$ exhibits greater selectivity, predominantly engaging with organic compounds through the electron transfer pathway. In contrast, $^\bullet$OH is characterized by non-selective reactivity, involving electrophilic addition to π bonds in unsaturated hydrocarbons and aromatics, hydrogen abstraction in aliphatic hydrocarbons, and electron transfers in halogenated hydrocarbons [131].

$SO_4^{\bullet-}$ presents higher energy barriers and greater selectivity in comparison to $^\bullet$OH owing to the steric hindrance associated with their relatively larger molecular size [132]. Consequently, the degradation of organic compounds through HR-AOPs and SR-AOPs yields notably distinct degradation by-products. In a study conducted by Chen et al. [133], the examination of the interaction between both $^\bullet$OH and $SO_4^{\bullet-}$ with phenol in the presence of nitrite was undertaken. Their findings revealed that the conversion of phenol to nitrophenol was significantly enhanced by $SO_4^{\bullet-}$ (47.5 %) in contrast to $^\bullet$OH (5.3 %). Intriguingly, the formation of nitrated phenols resulted in a remarkable 860 % increase in mutagenicity. In a study by Matta et al., it was reported that SRs ($SO_4^{\bullet-}$) resulted in more rapid degradation of carbamazepine in both aqueous solutions and real urban wastewater when compared to $^\bullet$OH. The authors suggested that $SO_4^{\bullet-}$ may exhibit greater selectivity than $^\bullet$OH in the oxidation of carbamazepine and could potentially serve as an intriguing alternative in advanced oxidation technologies (AOTs) for treating real urban wastewater [134].

Deng and Ezyske [135] highlighted the advantages of SR-AOTs over HR-AOTs, pointing out that $^\bullet$OH exhibit minimal reactivity toward the oxidation of ammonia. Furthermore, when compared to the Fenton treatment applied to the same batch leachate sample, thermal PS oxidation achieved a higher chemical oxygen demand (COD) removal rate, reaching 91 % (with $S_2O_8^{2-}$ dosage at 12 times the initial COD, at pH 4.0). In comparison, the Fenton treatment achieved a COD removal of 40 % (with H_2O_2 dosage at 2.125 times the initial COD, at pH 3.0), despite both treatments employing the same chemical dose. In their research, Ji et al. observed that $SO_4^{\bullet-}$ engages in the attachment of nitrophenols through denitration and renitration mechanisms [131]. Conversely, the $^\bullet$OH-mediated degradation of nitrophenols leads to the substitution of hydro and nitro groups by OH$^-$, yielding dihydroxynitro benzenes and polyhydroxylated benzenes [136]. In the context of propranolol degradation through UV/H_2O_2 and UV/PS processes, an acute toxicity assay employing *Vibrio fischeri* indicated that $SO_4^{\bullet-}$-mediated degradation in the UV/PS process resulted in the formation of more toxic by-products than $^\bullet$OH-mediated degradation [137]. Thus, it is imperative to thoroughly examine the potential toxic by-products associated with SR-AOPs before their practical implementation.

8 Mineralization/Degradation of Pollutants by PS/PMS-based on Activation Route

In their study, Crincoli et al. conducted a comparative analysis of the heterogeneous UV-activation of PS and H_2O_2 for the degradation of Rhodamine B (RhB). They observed that H_2O_2 activation exhibited a high reaction rate and was more cost-effective (H_2O_2: \$0.031 mol^{-1} vs. PS: \$0.24 mol^{-1}) in comparison to PS activation [138]. However, it is noteworthy that the high scavenging rate of H_2O_2 may lead to nonproductive consumption, potentially diminishing the radical reactions with the target compounds. Furthermore, the O—O bond dissociation energy of PS was determined to be 140 kJ mol^{-1}, significantly lower than that of H_2O_2 (213 kJ mol^{-1}) and ozone (O_3) (364 kJ mol^{-1}) [45]. These findings collectively favor the utilization of lower PS concentrations, compared to H_2O_2 to achieve equivalent treatment efficiency.

Escobedo et al. investigated involving the electrochemical activation of H_2O_2 and PS for two distinct water quality scenarios: water contaminated with heavy metals and real wastewater. In the case of water contaminated with heavy metals, counteracting the adverse influence of heavy metals on $^{\bullet}$OH induced mineralization necessitated the use of a higher quantity of H_2O_2 (91.1 mM) and a higher current density (45 $mA.cm^{-2}$), in contrast to PS activation, which required 25 mM of PS and a current density of 24.4 $mA.cm^{-2}$ [139]. Conversely, when dealing with real wastewater, the electrochemical activation of PS demonstrated superior TOC removal, reaching levels of 70–75 % within a 3-h period. However, this approach incurred certain drawbacks, including elevated effluent toxicity and relatively higher operational costs, primarily attributed to the substantial requirement for oxidants (totaling \$85 m^{-3}). In comparison, the electrochemical activation of H_2O_2 proved to be a more favorable option due to its lower toxicity and reduced operational costs (\$63 m^{-3}, mainly stemming from electricity consumption) [139].

Hori et al. researched on the mineralization of perfluorocarboxylic acids using PS activation, noting that the process was more effective at 80 °C, compared to 150 °C. Mineralization, as determined by CO_2 production, reached 37 % after 6 h for PS activated at 150 °C, while the corresponding mineralization was significantly higher at 70 % when conducted at 80 °C. This study subjected samples to the required reaction temperatures within an oven. Hori et al. explained the limited mineralization observed at high temperatures, attributing it to the potential increased production of $^{\bullet}$OH from $SO_4^{\bullet-}$ and the gasification of the pollutant and intermediates [140].

Lee et al. studied the degradation and mineralization of perfluorocarboxylic acids using microwave heating for PS activation. They investigated various temperature conditions, specifically at 60, 90, and 130 °C [141]. Similar to the findings, some researchers observed limited mineralization at 130 °C, compared to the oxidation of the pollutant at 90 °C. After 4 h of oxidation, mineralization at 130 °C reached only 40 %, whereas approximately 60 % and around 70 % mineralization were achieved at 60 and 90 °C, respectively. Subsequently, after 12 h, mineralization at 130 °C remained at 40 %, while approximately 80 % mineralization was attained at both 60 and 90 °C.

However, a bench-scale study conducted by Ferreira et al. presented a comparison of the efficacy of inactivated PS and chelated-Fe-activated PS for the remediation of anthracene-contaminated oxisol. They reported a remarkable 96 % degradation of the pollutant after 90 days for inactivated PS, whereas chelated-Fe-activated PS resulted in 70 % degradation of the pollutant over the same period. These findings suggest that inactivated PS may offer an effective means of pollutant degradation for specific applications, particularly when not under emergency conditions [142].

Furthermore, bench-scale studies ascertain the most appropriate AOPs for remediating an underground contaminated site have indicated that inactivated PS represents a highly competitive technique. In the realm of pollutant degradation, inactivated PS surpassed base-activated PS treatment and can be considered to have outperformed all other techniques examined in the study in terms of requiring the least amount of oxidant consumption [143].

Sra et al. presented a case where the treatment of a gasoline source zone was carried out by injecting inactivated PS, and the monitoring spanned for more than 10 months. The outcomes revealed a notable reduction in gasoline components, ranging from 52 % to 86 %, within the monitoring wells between 60 and 80 days from the commencement of the remediation effort [144]. However, it is worth noting that the cumulative reduction in the targeted pollutants over 315 days was comparatively smaller, falling within the range of 19 % to 58 %. The earlier substantial reductions in pollutant levels were attributed, in part, to dilution resulting from the injection of the PS solution. It should be noted that the PS was effectively consumed within approximately 100 days. For an effective pollutant degradation, it is recommended to replenish the PS at prescribed intervals [144].

9 Conclusion

The need for pharmaceutical products appears inevitable due to imminent demands for their use by plants, livestock, and humans, as a means to either improve or maintain one health condition or the other. Hence, it is estimated that their occurrence in wastewater may continue to be on the high side due to this. However, the use of conventional treatment methods removing pharmaceutical ingredients has not achieved much success, compared to advanced oxidation methods. PS or PMS is a potential precursor for advanced oxidation processes. However, its oxidative potential is enhanced when both physical and chemical activation approaches activate it. As an oxidizing agent, it largely enhances photocatalytic degradation of pharmaceutical contaminants in water when it is used to dope photocatalysts. However, the dosage used would largely influence the extent of photodegradation as much as the dosage of photocatalysts and other factors would affect the degradation process. While UV radiations, ozone, and ultrasound systems have been embraced for the activation of PS and PMS, they may not be sustainable as they are costly and not environmentally friendly. Hence, there is a need for future research to consider looking into developing more green and sustainable methods for the activation of PS or PMS to facilitate advanced oxidation processes.

Conflicts of interest

The authors declare no conflict of interest.

Excel O. Anjorin is a lecturer in the Department of Integrated Science Education, Federal College of Education (Technical) Akoka, Lagos, Nigeria. He holds a B.Sc. (honors) in chemistry from the University of Ibadan, Ibadan, Nigeria, and an M.Sc. in Environmental and Analytical Chemistry from Redeemer's University, Ede, Nigeria.

Moses O. Alfred is a lecturer in the Department of Chemical Sciences, Redeemer's University, Ede, Nigeria. He holds a B.Sc. (honors) in industrial chemistry from Adekunle Ajasin University, Akungba-Akoko, Nigeria, an M.Sc. in environmental and analytical chemistry, and a Ph.D. in industrial chemistry, both from Redeemer's University, Ede, Nigeria. The focus of his research is the preparation and characterization of solar-active photocatalytic materials for the degradation of emerging contaminants in water, using local materials and agrowastes. He is a faculty member of the African Centre of Excellence for Water and Environment Research (ACEWATER), Redeemer's University, Ede, Nigeria.

Babajide Sotunde holds a B.Sc. (honors) in chemical engineering and an M.Sc. in chemical engineering, both from Obafemi Awolowo University, Ile-Ife, Nigeria. Currently, he is a Ph.D. student in the Department of Chemical Sciences and African Centre of Excellence for Water and Environment Research (ACEWATER), Redeemer's University, Ede, Nigeria. The focus of his research is syntheses and applications of functional biopolymers-photoactive materials for upscale treatment of emerging contaminants in water.

Esther A. Nnamani holds a B.Sc. (honors) in chemistry from the University of Ilorin, Ilorin, Nigeria, and an M.Sc. in industrial chemistry from Covenant University, Ota, Nigeria. Currently, she is a Ph.D. student in the Department of Chemical Sciences and African Centre of Excellence for Water and Environment Research (ACEWATER), Redeemer's University, Ede, Nigeria. The focus of her research is the environmental profiling, assessment, and remediation of emerging contaminants in environmental water using photoactive materials.

Ajibola A. Bayode is a lecturer in the Department of Chemical Sciences, Redeemer's University, Ede, Nigeria. She holds a B.Sc. (honors) in industrial chemistry from Achievers University, Owo, Nigeria, an M.Sc. in environmental and analytical chemistry, and a Ph.D. in industrial chemistry, both from Redeemer's University, Ede, Nigeria. The focus of her research is the syntheses of sustainable functional materials with applications in water treatment and clean energy generation.

Emmanuel I. Unuabonah is a professor in the Department of Chemical Sciences, Redeemer's University, Ede, Nigeria. He holds a B.Sc. (honors) in industrial chemistry from the University of Benin, Benin City, Nigeria, an M.Sc. in industrial chemistry, and a Ph.D. in chemistry from the University of Ibadan, Ibadan, Nigeria. The focus of his research is the preparation and characterization of functional composite materials from local materials and agrowastes with the aim of treating water. He is also developing novel micro-mesoporous materials for adsorptive and photocatalytic purposes.

Brigitte Helmreich is a professor at the Chair of Urban Water Systems Engineering, Technical University of Munich (TUM), Munich, Germany. She holds a Ph.D. from the Institute for Organic Chemistry, TUM, Munich, Germany. The focus of her research interest is multifunctional infiltration swales in residential areas, recycled soils and substrates, complexation of biocides and heavy metals, decentralized sustainable urban drainage systems, etc.

Martins O. Omorogie is a senior lecturer in the Department of Chemical Sciences, Redeemer's University, Ede, Nigeria. He holds a B.Sc. (honors) in industrial chemistry from the University of Benin, Benin City, Nigeria, an M.Sc. in physical chemistry, and a Ph.D. in chemistry from the University of Ibadan, Ibadan, Nigeria. The focus of his research is the syntheses, adsorptive, and catalytic applications of sustainable low-cost functional materials for the cleanup of emerging contaminants in water.

Acknowledgments

Dr. Martins O. Omorogie and Prof. Dr. Brigitte Helmreich are immensely grateful to the Alexander von Humboldt Foundation and the Carl Friedrich von Siemens Foundation for the award of Research Fellowship for Experienced Researcher to Dr. Martins O. Omorogie (NGA-1201082-HFST-E).

Open access funding enabled and organized by Projekt DEAL.

Abbreviations

–	[μs]	Microsecond
–	[ns]	Nanosecond
APIs	[–]	Active pharmaceuticals ingredients
WWT	[–]	Wastewater treatment plants
AOPs	[–]	Advanced oxidation processes
SR-AOPs	[–]	Sulfate radical-AOPs
REDOX	[–]	Reduction–oxidation
–	[V]	Volts
E°	[V$_{\text{NHE}}$]	Volts at normal hydrogen electrode
–	[W m^{-2}]	Watts per square meter
Dissociation energy	[kJ mol^{-1}]	Kilojoules per mole
Molar absorption coefficient	[M^{-1}.cm^{-1}]	Per (molar centimeter)
pKa	[M^{-1}.s $^{-1}$]	Molar per second
$h\nu$	[−]	Ultraviolet radiation
Temperature	[K or $^{\circ}$C]	Kelvin or degree celsius
ROS	[–]	Reactive oxygen species
HOMO	[–]	Highest occupied molecular orbital
LUMO	[–]	Lowest unoccupied molecular orbital
–	[nm]	Nanometer
LMCT	[–]	Ligand-to-metal charge transfer
BPA	[–]	Bisphenol A
CB	[–]	Conduction band
HA	[–]	Humic acid
pHpzc	[–]	Point of zero charge
NOM	[–]	Natural organic matter
ATZ	[–]	Atrazine
–	[mg L^{-1}]	Milligrams per liter
k_{obs}	[−]	Observed rate constant
SD	[–]	Sulfadiazine
PMS	[–]	Peroxymonosulfate
RhB	[–]	Rhodamine B
IBP	[–]	Ibuprofen
AO7	[–]	Acid Orange 7
HR	[–]	Hydroxyl radical
UV	[–]	Ultraviolet
MOF	[–]	Metal organic framework
Radical concentration	[L.mg.C^{-1}.s $^{-1}$]	Liter milligrams per (Coulomb second)
TOC	[–]	Total organic carbon
–	[mM]	Millimolar
Current density	[mA.cm^{-2}]	Milliampere per square centimeter
TTC	[–]	Tetracycline

References

[1] A. Sangion, P. Gramatica, *Environ. Int.* **2016**, *95*, 131–143.
[2] D. Destrieux, F. Laurent, H. Budzinski, J. Pedelucq, P. Vervier, M. Gerino, *Sci. Total Environ.* **2017**, *609*, 927–941.
[3] A. Causanilles, C. Ruepert, M. Ibáñez, E. Emke, F. Hernández, P. De Voogt, *Sci. Total Environ.* **2017**, *599*, 98–107.
[4] H. Lin, H. Li, L. Chen, L. Li, L. Yin, H. Lee, Z. Yang, *Ecotoxicol. Environ. Saf.* **2018**, *147*, 530–536.
[5] B. Gworek, M. Kijenska, J. Wrzosek, M. Granieswska, *Water Air. Soil. Pollut.* **2021**, *232* (4), 145.
[6] M. Biel-Maeso, C. Corada-Fernández, P. A. Lara-Martín, *Environmen. Pollut.* **2018**, *235*, 312–321.
[7] A. Ginebreda, D. Barceló, S. Rodríguez-Mozaz, in *Removal and Degradation of Pharmaceutically Active Compounds in Wastewater Treatment* (Eds: S. Rodriguez-Mozaz, P. B. Cano, M. S. Adroguer), Springer, Cham **2020**.
[8] J. Xiang, M. Wu, J. Lei, C. Fu, J. Gu, G. Xu, *Ecotoxicol. Environ. Saf.* **2018**, *150*, 289–296.
[9] R. Mirzaei, M. Yunesian, S. Nasseri, M. Gholami, E. Jalilzadeh, S. Shoeibi, A. Mesdaghinia, *Sci. Total Environ.* **2018**, *619*, 446–459.
[10] D. Kanakaraju, B. D. Glass, M. Oelgemöller, *J. Environ. Manage* **2018**, *219*, 189–207.
[11] S. C. Ameta, in *Advanced Oxidation Processes for Wastewater Treatment: Emerging Green Chemical Technology*, Elsevier, Amsterdam **2018**.
[12] S. Yang, P. Wu, J. Liu, M. Chen, Z. Ahmed, N. Zhu, *Chem. Eng. J.* **2018**, *350*, 484–495.
[13] X. Li, R. Chen, X. Long, H. Chen, M. Liu, Y. Du, S. Yang, Z. Qian, Y. Chen, D. Ding, *Sep. Purif. Technol.* **2023**, *327*, 124990.

[14] C. Cai, H. Zhang, X. Zhong, L. Hou, *J. Hazard. Mater.* **2015**, *283*, 70–79.
[15] W. Li, P.-X. Wu, Y. Zhu, Z.-J. Huang, Y.-H. Lu, Y.-W. Li, Z. Dang, N.-W. Zhu, *Chem. Eng. J.* **2015**, *279*, 93–102.
[16] W. Yang, Z. Jiang, X. Hu, X. Li, H. Wang, R. Xiao, *Chemosphere* **2019**, *220*, 514–522.
[17] T. Rajaraman, V. Gandhi, S. Parikh, in *Advances in Wastewater Treatment I* (Eds: V. Gandhi, K. Shah), Materials Research Forum, Millersville **2021**, 37–86.
[18] L. Liu, Z. Chen, J. Zhang, D. Shan, Y. Wu, L. Bai, B. Wang, *J. Water Process Eng.* **2021**, *42*, 102122.
[19] Z. Honarmandrad, X. Sun, Z. Wang, M. Naushad, G. Boczkaj, *Water Resour. Ind.* **2023**, *29*, 100194.
[20] L. Wang, K. Xiao, H. Zhao, *Water Res.* **2023**, *235*, 119925.
[21] R. R. Solís, I. F. Mena, M. N. Nadagouda, D. D. Dionysiou, *J. Hazard. Mater.* **2020**, *384*, 121340.
[22] C. Tan, N. Gao, Y. Deng, J. Deng, S. Zhou, J. Li, X. Xin, *J. Hazard. Mater.* **2014**, *276*, 452–460.
[23] J. R. De Andrade, M. G. A. Vieira, M. G. C. Da Silva, S. Wang, *Chem. Eng. J.* **2020**, *382*, 122971.
[24] S. Guerra-Rodríguez, E. Rodríguez, D. N. Singh, J. Rodríguez-Chueca, *Water Res.* **2018**, *10* (*12*), 1828.
[25] B.-T. Zhang, Y. Zhang, Y. Teng, M. Fan, *Crit. Rev. Environ. Sci. Technol.* **2015**, *45* (*16*), 1756–1800.
[26] F. Ghanbari, M. Moradi, *Chem. Eng. J.* **2017**, *310*, 41–62.
[27] C. Liang, C. Bruell, *Ind. Eng. Chem. Res.* **2008**, *47* (*9*), 2912–2918.
[28] Y. Deng, R. Zhao, *Curr. Pollut. Rep.* **2015**, *1*, 167–176.
[29] H. Marshall, *J. Chem. Soc., Trans.* **1891**, *59*, 760–771.
[30] G. P. Anipsitakis, D. D. Dionysiou, *Environ. Sci. Technol.* **2003**, *37* (*20*), 4790–4797.
[31] N. Jaafarzadeh, M. Omidinasab, F. Ghanbari, *Process Saf. Environ. Prot.* **2016**, *102*, 462–472.
[32] S. Giannakis, K.-Y. A. Lin, F. Ghanbari, *Chem. Eng. J.* **2021**, *406*, 127083.
[33] A. Hassani, J. Scaria, F. Ghanbari, P. Nidheesh, *Environ. Res.* **2022**, *217*, 114789.
[34] J. Scaria, P. V. Nidheesh, *Curr. Opin. Chem. Eng.* **2022**, *36*, 100830.
[35] X.-H. Yi, T.-Y. Wang, H.-Y. Chu, Y. Gao, C.-C. Wang, Y.-J. Li, L. Chen, P. Wang, H. Fu, C. Zhao, W. Liu, *Chem. Eng. J.* **2022**, *449*, 137784.
[36] A. Durán, J. M. Monteagudo, I. San Martín, F. J. Amunategui, D. A. Patterson, *Chemosphere* **2017**, *186*, 177–184.
[37] T. Xi, X. Li, Q. Zhang, N. Liu, S. Niu, Z. Dong, C. Lyu, *Front. Environ. Sci. Eng.* **2021**, *15*, 1–11. DOI: https://doi.org/10.1007/s11783-020-1347-5
[38] W.-D. Oh, Z. Dong, T.-T. Lim, *Appl. Catal., B* **2016**, *194*, 169–201.
[39] M. Ma, L. Chen, J. Zhao, W. Liu, H. Ji, *Chin. Chem. Lett.* **2019**, *30* (*12*), 2191–2195.
[40] H. Ferkous, S. Merouani, O. Hamdaoui, C. Pétrier, *Ultrason. Sonochem.* **2017**, *34*, 580–587.
[41] Y. Wei, Y. Gong, X. Zhao, Y. Wang, R. Duan, C. Chen, W. Song, J. Zhao, *Environ. Sci.: Nano* **2019**, *6* (*5*), 1585–1593.
[42] X. Xia, F. Zhu, J. Li, H. Yang, L. Wei, Q. Li, J. Jiang, G. Zhang, Q. Zhao, *Front. Chem.* **2020**, *8*, 592056.
[43] Y. Wang, X. Zhao, D. Cao, Y. Wang, Y. Zhu, *Appl. Catal., B* **2017**, *211*, 79–88.
[44] S. Xiao, M. Cheng, H. Zhong, Z. Liu, Y. Liu, X. Yang, Q. Liang, *Chem. Eng. J.* **2020**, *384*, 123265.
[45] S. Wacławek, H. V. Lutze, K. Grübel, V. V. T. Padil, M. Černík, D. D. Dionysiou, *Chem. Eng. J.* **2017**, *330*, 44–62.
[46] J. Wang, S. Wang, *Chem. Eng. J.* **2018**, *334*, 1502–1517.
[47] J. Peng, H. Zhou, W. Liu, Z. Ao, H. Ji, Y. Liu, S. Su, G. Yao, B. Lai, *Chem. Eng. J.* **2020**, *397*, 125387.
[48] Y. Zhou, J. Jiang, Y. Gao, J. Ma, S.-Y. Pang, J. Li, X.-T. Lu, L.-P. Yuan, *Environ. Sci. Technol.* **2015**, *49* (*21*), 12941–12950.
[49] G. Matafonova, V. Batoev, *Water Res.* **2018**, *132*, 177–189.
[50] V. R. Battula, A. Jaryal, K. Kailasam, *J. Mater. Chem. A* **2019**, *7* (*10*), 5643–5649.
[51] J. Lee, U. Von Gunten, J.-H. Kim, *Environ. Sci. Technol.* **2020**, *54* (*6*), 3064–3081.
[52] I. A. Ike, K. G. Linden, J. D. Orbell, M. Duke, *Chem. Eng. J.* **2018**, *338*, 651–669.
[53] L. Zhou, X. Yang, Y. Ji, J. Wei, *Sci. Total Environ.* **2019**, *692*, 201–208.
[54] Y. Ji, Y. Shi, W. Dong, X. Wen, M. Jiang, J. Lu, *Chem. Eng. J.* **2016**, *298*, 225–233.
[55] I. A. Ike, J. D. Orbell, M. Duke, *Chem. Eng. Res. Des.* **2018**, *136*, 304–314.
[56] Z.-H. Huang, Z.-Y. Ji, Y.-Y. Zhao, J. Liu, F. Li, J.-S. Yuan, *Chem. Eng. J.* **2020**, *380*, 122411.
[57] H. A. El-monem, H. Mahanna, M. El-Halwany, M. Samy, *Environ. Sci. Pollut. Res. Int.* **2024**, *31*, 24153–24162.
[58] Y. Chen, M. Li, Y. Tong, Z. Liu, L. Fang, Y. Wu, Z. Fang, F. Wu, L.-Z. Huang, *Chem. Eng. J.* **2019**, *368*, 495–503.
[59] X. Ao, W. Liu, W. Sun, M. Cai, Z. Ye, C. Yang, Z. Lu, C. Li, *Chem. Eng. J.* **2018**, *345*, 87–97.
[60] J. C. Carlson, M. I. Stefan, J. M. Parnis, C. D. Metcalfe, *Water Res.* **2015**, *84*, 350–361.
[61] H. Guo, X. Zhou, Y. Zhang, Q. Yao, Y. Qian, H. Chu, J. Chen, *J. Environ. Sci.* **2020**, *91*, 10–21.
[62] C. Zhu, F. Liu, C. Ling, H. Jiang, H. Wu, A. Li, *Appl. Catal., B* **2019**, *242*, 238–248.
[63] L. W. Matzek, K. E. Carter, *Chemosphere* **2016**, *151*, 178–188.
[64] C. Von Sonntag, *Water Sci. Technol.* **2008**, *58* (*5*), 1015–1021.
[65] S. Nasseri, A. H. Mahvi, M. Seyedsalehi, K. Yaghmaeian, R. Nabizadeh, M. Alimohammadi, G. H. Safari, *J. Mol. Liq.* **2017**, *241*, 704–714.
[66] C. Qi, X. Liu, J. Ma, C. Lin, X. Li, H. Zhang, *Chemosphere* **2016**, *151*, 280–288.
[67] P. Devi, U. Das, A. K. Dalai, *Sci. Total Environ.* **2016**, *571*, 643–657.
[68] D. Zhao, X. Liao, X. Yan, S. G. Huling, T. Chai, H. Tao, *J. Hazard. Mater.* **2013**, *254*, 228–235.
[69] J. Yang, M. Zhu, D. D. Dionysiou, *Water Res.* **2021**, *189*, 116627.
[70] S. Yang, P. Wang, X. Yang, L. Shan, W. Zhang, X. Shao, R. Niu, *J. Hazard. Mater.* **2010**, *179* (*1-3*), 552–558.
[71] K. H. Chan, W. Chu, *Water Res.* **2009**, *43* (*9*), 2513–2521.
[72] X. Chen, X. Qiao, D. Wang, J. Lin, J. Chen, *Chemosphere* **2007**, *67* (*4*), 802–808.
[73] C. Marinescu, M. Ben Ali, A. Hamdi, Y. Cherifi, A. Barras, Y. Coffinier, S. Somacescu, V. Raditoiu, S. Szunerits, R. Boukherroub, *Chem. Eng. J.* **2018**, *336*, 465–475.
[74] Y. Zhu, R. Zhu, Y. Xi, J. Zhu, G. Zhu, H. He, *Appl. Catal., B* **2019**, *255*, 117739.
[75] C. Liang, Z.-S. Wang, N. Mohanty, *Sci. Total Environ.* **2006**, *370* (*2-3*), 271–277.
[76] Y. Xue, W. Dong, X. Wang, W. Bi, P. Zhai, H. Li, M. Nie, *Environ. Sci. Pollut. Res.* **2016**, *23*, 4561–4568.

[77] Y. Xue, W. Dong, X. Wang, W. Bi, P. Zhai, H. Li, M. Nie, *Environ. Sci. Pollut. Res. Int.* **2016**, *23*, 4561–4568.
[78] H. Mahanna, N. El-Bendary, *Int. J. Environ. Sci. Technol.* **2022**, *19* (*11*), 10945–10956.
[79] L. A. Achola, A. Ghebrehiwet, J. Macharia, P. Kerns, J. He, J. Fee, C. Tinson, J. Shi, S. March, M. Jain, S. L. Suib, *Appl. Catal., B* **2020**, *263*, 118332.
[80] Y. Gao, Z. Zhang, S. Li, J. Liu, L. Yao, Y. Li, H. Zhang, *Appl. Catal., B* **2016**, *185*, 22–30.
[81] Y. Jo, C. Kim, G.-H. Moon, J. Lee, T. An, W. Choi, *Chem. Eng. J.* **2018**, *346*, 249–257.
[82] G. Zhang, G. Kim, W. Choi, *Energy Environ. Sci.* **2014**, *7* (*3*), 954–966.
[83] Y. Wu, A. Bianco, M. Brigante, W. Dong, P. de Sainte-Claire, K. Hanna, G. Mailhot, *Environ. Sci. Technol.* **2015**, *49* (*24*), 14343–14349.
[84] M. M. Ahmed, S. Chiron, *Water Res.* **2014**, *48*, 229–236.
[85] S. Miralles-Cuevas, I. Oller, A. Ruíz-Delgado, A. Cabrera-Reina, L. Cornejo-Ponce, S. Malato, *J. Hazard. Mater.* **2019**, *372*, 129–136.
[86] L. Yang, L. He, J. Xue, Y. Ma, Z. Xie, L. Wu, M. Huang, Z. Zhang, *J. Hazard. Mater.* **2020**, *393*, 122405.
[87] R. Hazime, Q. H. Nguyen, C. Ferronato, T. K. X. Huynh, F. Jaber, J.-M. Chovelon, *Appl. Catal., B* **2013**, *132*, 519–526.
[88] H. Ding, J. Hu, *Chem. Eng. J.* **2020**, *397*, 125462.
[89] L. Yang, L. Xu, X. Bai, P. Jin, *J. Hazard. Mater.* **2019**, *365*, 107–117.
[90] L. Yang, X. Bai, J. Shi, X. Du, L. Xu, P. Jin, *Appl. Catal., B* **2019**, *256*, 117759.
[91] S. Bekkouche, S. Merouani, O. Hamdaoui, M. Bouhelassa, *J. Photochem. Photobiol. A: Chem.* **2017**, *345*, 80–91.
[92] J. Wang, X. Liu, Y. Li, T. Powell, X. Wang, G. Wang, P. Zhang, *Sci. Total Environ.* **2019**, *691*, 848–857.
[93] A. A. Babaei, M. Golshan, B. J. P. S. Kakavandi, *E. Protection*, **2021**, *149*, 35–47.
[94] T. Zhang, Y. Liu, Y. Rao, X. Li, D. Yuan, S. Tang, Q. Zhao, *Chem. Eng. J.* **2020**, *384*, 123350.
[95] Y. Rao, Y. Zhang, A. Li, T. Zhang, T. Jiao, *Chemosphere* **2021**, *266*, 129236.
[96] Q. Li, L. Wang, L. Zhang, H. Xie, *Res. Chem. Intermed.* **2019**, *45*, 757–768.
[97] M. Golshan, B. Kakavandi, M. Ahmadi, M. Azizi, *J. Hazard. Mater.* **2018**, *359*, 325–337.
[98] A. A. Babaei, M. Golshan, B. Kakavandi, *Process Saf. Environ. Prot.* **2021**, *149*, 35–47.
[99] J. Monteagudo, A. Durán, I. San Martín, B. Vellón, *Sep. Purif. Technol.* **2020**, *238*, 116456.
[100] L. Ismail, C. Ferronato, L. Fine, F. Jaber, J.-M. Chovelon, *Appl. Catal., B* **2017**, *201*, 573–581.
[101] M. R. Eskandarian, M. H. Rasoulifard, M. Fazli, L. Ghalamchi, H. Choi, *Korean J. Chem. Eng.* **2019**, *36*, 965–974.
[102] S. Jorfi, B. Kakavandi, H. R. Motlagh, M. Ahmadi, N. Jaafarzadeh, *Appl. Catal., B* **2017**, *219*, 216–230.
[103] Q. Li, L. Wang, X. Fang, L. Zhang, J. Li, H. Xie, *Catalysts* **2019**, *9* (*2*), 189.
[104] X. Du, X. Bai, L. Xu, L. Yang, P. Jin, *Chem. Eng. J.* **2020**, *384*, 123245.
[105] J. Jia, D. Liu, S. Wang, H. Li, J. Ni, X. Li, J. Tian, Q. Wang, *Sep. Purif. Technol.* **2020**, *253*, 117510.
[106] C. Liang, H.-W. Su, *Ind. Eng. Chem. Res.* **2009**, *48* (*11*), 5558–5562.
[107] B. Xu, M. B. Ahmed, J. L. Zhou, A. Altaee, *Chemosphere* **2020**, *243*, 125366.
[108] S. Xiao, M. Cheng, H. Zhong, Z. Liu, Y. Liu, X. Yang, Q. Liang, **2020**, *384*, 123265. DOI: https://doi.org/10.1016/j.cej.2019.123265
[109] J. Wang, S. Wang, *Chem. Eng. J.* **2021**, *411*, 128392.
[110] G.-D. Fang, D. D. Dionysiou, Y. Wang, S. R. Al-Abed, D.-M. Zhou, *J. Hazard. Mater.* **2012**, *227*, 394–401.
[111] S. Wang, N. Zhou, S. Wu, Q. Zhang, Z. Yang, *Ultrason. Sonochem.* **2015**, *23*, 128–134.
[112] A. Fawzy, H. Mahanna, M. Mossad, *Environ Sci Pollut Res Int* **2022**, *29* (*45*), 68532–68546.
[113] F. Jabbari, A. Eslami, J. Mahmoudian, *Health Scope* **2020**, *9* (*2*), e99436.
[114] W. Qin, Z. Lin, L. Sun, X. Yuan, D. Xia, *Ozone: Sci. Eng.* **2020**, *42* (*6*), 558–564.
[115] R. Yin, W. Guo, H. Wang, J. Du, Q. Wu, J.-S. Chang, N. Ren, *Chem. Eng. J.* **2019**, *357*, 589–599.
[116] A. Seidmohammadi, G. Asgari, L. Torabi, *J. Mazandaran Univ. Med. Sci.* **2016**, *26* (*143*), 160–173.
[117] Y. Wu, S. Mao, C. Liu, F. Pei, F. Wang, Q. Hao, M. Xia, W. Lei, *J. Colloid Interface Sci.* **2022**, *608*, 322–333.
[118] Y.-Q. Gao, N.-Y. Gao, Y. Deng, Y.-Q. Yang, Y. Ma, *Chem. Eng. J.* **2012**, *195–196*, 248–253.
[119] X. Zou, T. Zhou, J. Mao, X. Wu, *Chem. Eng. J.* **2014**, *257*, 36–44.
[120] N. El-Bendary, H. K. El-Etriby, H. Mahanna, *Environ. Technol.* **2022**, *43* (*28*), 4438–4454.
[121] J. Zhao, Y. Wang, N. Li, S. Wang, J. Yu, X. Li, *Chemosphere* **2021**, *276*, 130257. DOI: https://doi.org/10.1016/j.chemosphere.2021.130257
[122] X. Wang, Y. Ding, D. D. Dionysiou, C. Liu, Y. Tong, J. Gao, G. Fang, D. Zhou, *Sci. Total Environ.* **2020**, *749* (*142387*), 142387.
[123] R. Xiao, L. Gao, Z. Wei, R. Spinney, S. Luo, D. Wang, D. D. Dionysiou, C.-J. Tang, W. Yang, *Environ. Pollut.* **2017**, *231*, 1446–1452.
[124] A. Fernandes, P. Makoś, G. Boczkaj, *J. Cleaner Prod.* **2018**, *195*, 374–384.
[125] L. Urán-Duque, J. C. Saldarriaga-Molina, A. Rubio-Clemente, *Water* **2021**, *13* (*17*), 2445.
[126] J. M. Jazić, T. Đurkić, B. Bašić, M. Watson, T. Apostolović, A. Tubića, J. Agbaba, *Environ. Sci.: Water Res. Technol.* **2020**, *6* (*10*), 2800–2815.
[127] C. Amor, J. R. Fernandes, M. S. Lucas, J. A. Peres, *Environ. Technol. Innov.* **2021**, *21*, 101183.
[128] T. Olmez-Hanci, I. Arslan-Alaton, *Chem. Eng. J.* **2013**, *224*, 10–16.
[129] K. Fedorov, M. Plata-Gryl, J. A. Khan, G. Boczkaj, *J. Hazard. Mater.* **2020**, *397*, 122804.
[130] Q. Zhong, Q. Lin, W. He, H. Fu, Z. Huang, Y. Wang, L. Wu, *Sep. Purif. Technol.* **2021**, *276*, 119354.
[131] Y. Ji, Y. Shi, Y. Yang, P. Yang, L. Wang, J. Lu, J. Li, L. Zhou, C. Ferronato, J.-M. Chovelon, *J. Hazard. Mater.* **2019**, *361*, 152–161.
[132] L. Gao, Q. Mao, S. Luo, L. Cao, X. Xie, Y. Yang, Y. Deng, Z. Wei, *Environ. Pollut.* **2020**, *259*, 113795.
[133] C. Chen, Z. Wu, S. Zheng, L. Wang, X. Niu, J. Fang, *Environ. Sci. Technol.* **2020**, *54* (*13*), 8455–8463.

[134] R. Matta, S. Tlili, S. Chiron, S. Barbati, *Environ. Chem. Lett.* **2011**, *9*, 347–353.
[135] Y. Deng, C. M. Ezyske, *Water Res.* **2011**, *45* (*18*), 6189–6194.
[136] Q. Mei, H. Cao, D. Han, M. Li, S. Yao, J. Xie, J. Zhan, Q. Zhang, W. Wang, M. He, *J. Hazard. Mater.* **2020**, *389*, 121901.
[137] Y. Yang, Y. Cao, J. Jiang, X. Lu, J. Ma, S. Pang, J. Li, Y. Liu, Y. Zhou, C. Guan, *Water Res.* **2019**, *149*, 543–552.
[138] K. Rusevova Crincoli, S. G. Huling, *Chem. Eng. J.* **2021**, *404*, 126404.
[139] E. Escobedo, K. Cho, Y.-S. Chang, *J. Hazard. Mater.* **2022**, *423*, 127068.
[140] H. Hori, Y. Nagaoka, M. Murayama, S. Kutsuna, *Environ. Sci. Technol.* **2008**, *42* (*19*), 7438–7443.
[141] Y.-C. Lee, S.-L. Lo, P.-T. Chiueh, D.-G. Chang, *Water Res.* **2009**, *43* (*11*), 2811–2816.
[142] I. D. Ferreira, T. Prieto, J. G. Freitas, N. R. Thomson, I. L. Nantes, E. J. H. Bechara, *Water, Air, Soil Pollut.* **2017**, *228*, 146.
[143] L. R. Bennedsen, in *Chemistry of Advanced Environmental Purification Processes of Water: Fundamentals and Applications* (Ed: E. Sogaard), Elsevier, Amsterdam **2014**.
[144] K. S. Sra, N. R. Thomson, J. F. Barker, *J. Contam. Hydrol.* **2013**, *150*, 35–44.
[145] Z. Zhang, H. Chen, J. Wang, Y. Zhang, *Radiat. Phys. Chem.* **2020**, *170*, 108639. DOI: https://doi.org/10.1016/j.radphyschem.2019.108639
[146] Y. Peng, H. Shi, Z. Wang, Y. Fu, Y. Liu, *RSC Adv.* **2021**, *11* (*12*), 6804–6817. DOI: https://doi.org/10.1039/d0ra10178h
[147] Y. Fu, X. Gao, J. Geng, S. Li, G. Wu, H. Ren, *Chem. Eng. J.* **2019**, *356*, 1032–1041. DOI: https://doi.org/10.1016/j.cej.2018.08.013
[148] A. Kontogiannis, E. Evgenidou, C. Nannou, D. Bikiaris, D. Lambropoulou, *J. Environ. Chem. Eng.* **2022**, *10* (*4*), 108112. DOI: https://doi.org/10.1016/j.jece.2022.108112